sustainability

MDPI

Article

Sequestration of Lead Ion in Aqueous Solution onto Chemically Pretreated *Pycnanthus angolensis* Seed Husk: Implications for Wastewater Treatment

Arinze Longinus Ezugwu [1,*], Hillary Onyeka Abugu [1], Ifeanyi Adolphus Ucheana [2], Samson Ifeanyi Eze [1], Johnbosco C. Egbueri [3], Victor Sunday Aigbodion [4] and Kovo Godfrey Akpomie [1,5]

[1] Department of Pure and Industrial Chemistry, University of Nigeria, Nsukka 410105, Enugu State, Nigeria; hillary.abugu@unn.edu.ng (H.O.A.); eze.samson@unn.edu.ng (S.I.E.); kovo.akpomie@unn.edu.ng (K.G.A.)
[2] Central Science Laboratory, University of Nigeria, Nsukka 410105, Enugu State, Nigeria; ifeanyi.ucheana@unn.edu.ng
[3] Department of Geology, Chukwuemeka Odumegwu Ojukwu University, Awka 432107, Uli Anambra State, Nigeria; johnboscoegbueri@gmail.com
[4] Faculty of Engineering and Built Environment, University of Johannesburg, Johannesburg 2092, South Africa; victor.aigbodion@unn.edu.ng
[5] Department of Chemistry, University of Free State, Bloemfontein 9301, South Africa
* Correspondence: arinze.ezugwu.192194@unn.edu.ng

Abstract: This novel study investigated and proposes the use of *Pycnanthus angolensis* seed husk for the sequestration of Pb(II) from contaminated solutions, with the aim of contributing to the urgent need for accessibility to quality water, sustainable management of water and the environment in line with the Sustainable Development Goals (SDGs). The activated *Pycnanthus angolensis* seed husk was developed by modifying the pure sample (P-PA) with ethylene-glycol (E-PA) and Iso-butanol (I-PA). Infrared spectroscopy (FTIR), scanning electron microscopy (SEM), the Brunauer-Emmett-Teller (BET) analyzer, thermogravimetric analyzer (TGA), and X-ray diffractometer (XRD) were used to characterize the adsorbents before and after adsorption. The batch adsorption studies carried out revealed the highest adsorption of Pb(II) at pH 6 and 180 min for all the adsorbents. The functional groups, as well as the shifts in peaks after modification, were confirmed using FTIR analysis. In addition, SEM images show a heterogeneous, rough surface with sufficient cavities of the adsorbent after modification. The physiochemical characteristics indicated that BET pore volume and pore diameter increased for E-PA and I-PA compared to P-PA. The experimental data obtained indicated that Langmuir and pseudo-first-order (PFO) best described the isotherm and kinetic models, respectively. The adsorption mechanism revealed that the adsorption of Pb(II) was controlled mainly by pore filling, while electrostatic interaction, surface complexation, and ionic exchange also occurred minimally. The thermodynamic parameters, ΔH° and ΔG°, suggest an endothermic and spontaneous adsorption process, respectively. The findings in this study indicate that *Pycnanthus angolensis* seed husks offer cost-effective and sustainable solutions that are readily accessible for wastewater treatment.

Keywords: biosorbent; adsorption mechanism; lead adsorption; error function; thermodynamics; *Pycnanthus angolensis*; chemical-treated biomass

Citation: Ezugwu, A.L.; Abugu, H.O.; Ucheana, I.A.; Eze, S.I.; Egbueri, J.C.; Aigbodion, V.S.; Akpomie, K.G. Sequestration of Lead Ion in Aqueous Solution onto Chemically Pretreated *Pycnanthus angolensis* Seed Husk: Implications for Wastewater Treatment. *Sustainability* **2023**, *15*, 15446. https://doi.org/10.3390/su152115446

Academic Editor: Said Muhammad

Received: 26 September 2023
Revised: 23 October 2023
Accepted: 25 October 2023
Published: 30 October 2023

1. Introduction

Recent reports have shown that heavy metals, even at a minimal concentration, could be detrimental to life forms [1–3]. Due to their highly toxic nature and their inability to undergo degradation, they have become a global concern and a major target for most scientists [4–6]. These metals have also been found in living cells [1]. Within living organisms, they tend to accumulate, binding to nucleic acids and proteins, thereby disrupting essential cellular functions and causing severe health consequences [1,7,8].

Lead (Pb) contamination has been listed as a major global concern due to its toxicity and negative impact on the human system [9–11]. It enters the environment primarily via the metal processing industries, chemical industries, mining, paint, and battery production processes [12–14]. Although there is a minimal level of Pb(II) in the surface water, when water is used without being purified, it accumulates in the environment [15]. More so, when substances contaminated with Pb(II) enter the food chain and are consumed at concentrations above the acceptable limit by plants or animals, it is detrimental to their health [16–18].

Among the different technologies used for wastewater treatment, adsorption has proven to be a reliable and environmentally friendly method [19–21]. Recent research has explored the use of agricultural and biological waste materials as adsorbents for removing metal ions from contaminated solutions. Notable examples include black cumin seed [22], *Terminalia mantaly* [23], fruit peels from banana, granadilla, and orange [24], peanut shells and compost [25], Ajwa Date Pits [26], and endocarp waste of Gayo Coffee [27]. These materials offer cost-effective and sustainable solutions that are readily accessible in large quantities [28,29]. Other reported adsorbents employed for the adsorption of contaminants are *Gigantochloa* bamboo [30], *Nepenthes rafflesiana* pitcher (NP), *Nepenthes rafflesiana* leaves [31], and modified waste shrimp shell (MSS) [32].

Previous reports showed that different functional groups on biomaterial surfaces are the driving factor in the removal of contaminants [33]. To improve its adsorption efficiency, researchers have used different modification methods (thermal, acid, base, and organic reagents) to address it. These modifications result in an increase in the biosorbents' pore cavities and enhance the number of oxygen-containing functional groups on the surface of the material, thereby improving its adsorption efficiency [34]. While many chemicals have been used for the modification of adsorbents [35–37], research is still scanty on the use of organic reagents to increase adsorption efficiency.

The *Pycnanthus angolensis* seed husk is widely called African nutmeg because of its close resemblance to nutmeg species seeds. It comes from a tropical plant in the *Myristicaceae* family and has been used to treat a wide range of health problems in Africa [38]. The fruits, which possess an oblong shape, consist of seeds abundant in oil content that are enclosed within a rigid outer shell [39]. The tree exhibits a substantial size, characterized by a diminutive crown consisting of branches positioned perpendicularly to the trunk [40]. In Nigeria, it is used in the treatment of chest pain, malaria, and bacterial infections [41]. This is because the seed contains bioactive compounds like quinone-terpenoids, lignans, isoflavonoids, kombic acid, tocochromanols, vitamins, and other compounds found in essential oils [38]. The *Pycnanthus angolensis* seed husk contains predominantly fat, carbohydrate, protein, and lignocellulosic materials (cellulose, hemicellose, and lignin), which are suitable materials for adsorption [29,31]. The structure of lignocellulose, tocochotrienol derivatives, and myristoleic acid contains sufficient (OH), (CO), (COOH), and (C=C) functional groups that could necessitate an effective removal process, thus necessitating this investigation for its potential as an adsorbent [16,42]. However, while this seed has been employed for medical applications [42] and for anti-malaria analysis [39], there has been no reported work on the use of *Pycnanthus angolensis* seed husk for the removal of contaminants in aqueous solutions.

Therefore, the goal of this work is to use *Pycnanthus angolensis* seed husk as an adsorbent to remove Pb(II) from aqueous solutions, activate some of the adsorbents with ethylene glycol and iso-butanol to improve its adsorption capacity and compare the adsorbents. The research also targets to characterize the prepared adsorbents using infrared spectroscopy (FTIR), scanning electron microscopy (SEM), the Brunauer-Emmett-Teller (BET) analyzer, thermogravimetric analyzer (TGA), and X-ray diffractometer (XRD). Finally, the research hopes to investigate the potential of the adsorbents for the sequestration of Pb(II) from wastewater. Lead contamination in aqueous environments poses a significant threat to both human health and ecosystems, demanding immediate attention. Traditional wastewater treatment methods often rely on non-renewable resources and can be energy-intensive,

presenting sustainability challenges. Thus, the justification for this research lies at the intersection of pressing environmental concerns [43,44], the need for sustainable solutions [45], and the promise of innovative and eco-friendly materials. With these critical issues in view, this study proposes the sequestration of lead ions using innovative and eco-friendly chemically modified *Pycnanthus angolensis* seed husk—a novel approach with multifaceted sustainability implications. The novelty of this present research centers around the application of this natural, renewable, and biodegradable material, the *Pycnanthus angolensis* seed husk, as an efficient adsorbent for lead ions.

2. Materials and Method

2.1. Adsorbent Preparation

The appropriate amount of sample required for the analysis was collected in line with the stipulated guidelines set by the Convention on International Trade in Endangered Species of Wild Fauna and Flora and was identified in the Plant Science and Biotechnology Department, University of Nigeria, Nsukka.

The seed husk was washed with clean water, sun-dried for 72 h, and subsequently pulverized to achieve a very fine particle size. The dried residue was sieved to get a homogenous size (diameter less than 1.0 to 250 µm). 100 g of the powdered seed husk was treated with 250 mL of iso-butanol for 48 h to get the iso-butanol-modified *Pycnanthus angolensis* (I-PA). 250 mL of ethylene glycol was also used to treat another 100 g of the powdered seed husk for 48 h, and the filtrate was labeled (E-PA) while another sample of powered, unmodified seed husk was labeled (P-PA). The samples were washed with de-ionized water, and the filtrate was tested several times until it became neutral. The residues were dried in an oven at 105 °C, allowed to cool, and stored in an airtight container. The dried samples were characterized to ascertain the impacts of organic solvent on the *Pycnanthus angolensis* seed husk on adsorption. A graphical illustration of this procedure is presented in Figure 1.

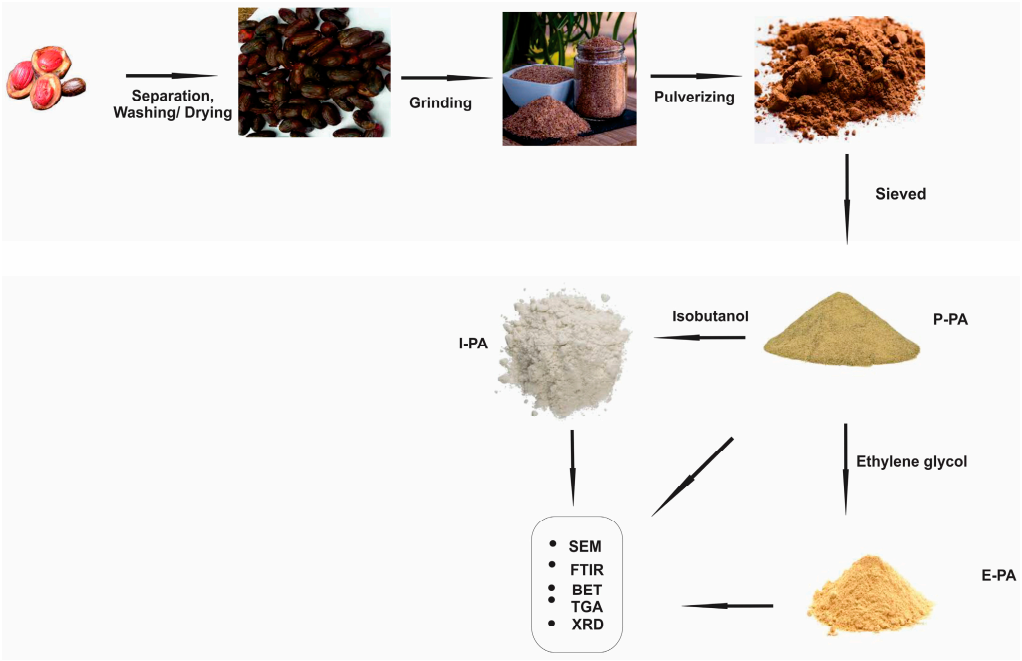

Figure 1. Flow chart of the adsorbent preparation procedure.

2.2. Characterization of Adsorbents

As shown in Figure 2, the samples were characterized using Fourier transform infrared spectroscopy (FTIR), scanning electron microscopy (SEM), the Brunauer-Emmett-Teller (BET) analyzer, the thermogravimetric analyzer (TGA), and an X-ray diffractometer (XRD). Fourier-transformed infrared spectroscopy (Perkin Elmer Spectrum 65 FT-IR spectropho-

tometer, Rodgau, Germany) was used to determine the functional groups present in the biosorbents, and the spectra were recorded in the range of 500–4000 cm^{-1}. The surface structure of the sorbent under different magnifications was obtained using scanning electron microscopy (SEM). The surface area, pore diameter, and pore sizes were investigated using the Brunauer-Emmett-Teller (BET) analyzer (JW-DA: 76502057en, Beijing, China). The Rigaku D/Max-llC X-ray diffractometer (Applied Rigaku Technologies, Cedar Park, TX, USA) was used to measure the XRD spectra of the modified adsorbents to determine their crystallinity, and the TGA was used to measure the thermal stability of the adsorbents.

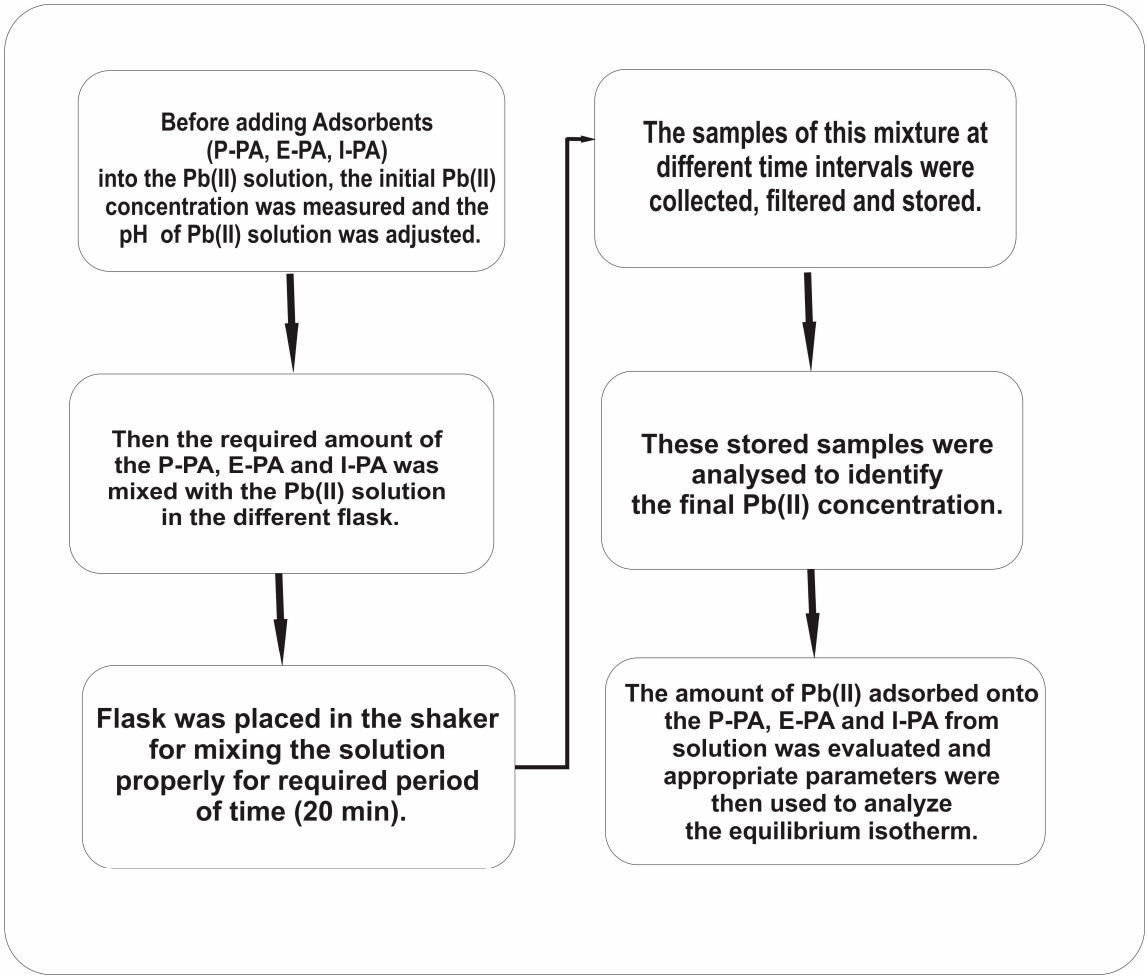

Figure 2. Experimental batch adsorption process.

2.3. Adsorbate Preparation and Models

2.3.1. Preparation and Dilution of $Pb(NO_3)_2$ Stock Solutions

A stock solution of Pb with a concentration of 1000 mg/L was made by dissolving 1.598 g of $Pb(NO_3)_2$ salt in a small amount of de-ionized water in a beaker and stirring it with a glass rod until the salt was completely dissociated. It was appropriately transferred into a 1 L volumetric flask and made up to the mark with de-ionized water. Several concentrations of synthetic wastewater containing lead (II) ions were later prepared using serial dilution.

2.3.2. Batch Adsorption Studies

In this work, the influence of the reaction conditions on the adsorption capacity of the prepared adsorbents for the uptake of lead was ascertained using the batch technique. 10 mL of the prepared adsorbate at different known concentrations were charged individually into five different beakers. I g of the adsorbents were accurately weighed and put

into each of the 250 mL beakers containing the adsorbate at a constant pH of 5 and room temperature. The beakers were put in a magnetic flask shaker at 100 rpm for 20 min to ensure adsorption efficiency was attained. After equilibrium was attained, these mixtures were filtered at various time intervals, and the filtrate was stored. The final concentration of Pb(II) was analyzed with an atomic absorption spectrometer. The quantity of Pb(II) ion uptake onto the P-PA, E-PA, and I-PA from mixtures was estimated, and the appropriate variables were employed to determine the isotherm and kinetic models. Figure 2 shows the breakdown of the experimental batch adsorption process.

2.3.3. Isotherm Models

Five isotherm models were used to evaluate the adsorption efficiency of the modified sorbents with the target metal ions [46]. This study was done using the linearized forms of the various models, such as Langmuir, Freundlich, and Temkin, the Dubinin–Radushkevich models, and Flory–Huggins models [47]. However, Langmuir and Freundlich models are mostly used for the adsorption of contaminants from aqueous solutions [48]. The summary of the parameters used for the isotherm and kinetic plots is presented in Table 1.

Table 1. Summary of parameters used for the Isotherm and Kinetic model linear plots.

Model	Plot	Equations
Langmuir	$\frac{C_e}{C_e}$ vs. C_e	(1)
Freundlich	ln q_e vs. ln C_e	(2)
Tempkin	q_e vs. ln C_e	(3)
	$B = \frac{RT}{b_T}$	(4)
D-R	ln q_e vs. ε^2	(5)
Florry Huggins	$\log(1-\theta)$ vs. $\log\left(\frac{\theta}{C_o}\right)$	(6)
PFO	$\log(q_{e,cal} - q_t)$ vs. t	(7)
PSO	$\frac{t}{q_t}$ vs. t	(8)
ID	q_t vs. $t^{0.5}$	(9)

2.3.4. Langmuir Isotherm Model

Langmuir predicts the monolayer adsorption mechanism of metal ions onto the sorbent surfaces [25]. The linearized equation of the Langmuir model (Equation (1)) was employed to evaluate the isotherm variables.

$$\frac{C_e}{q_e} = \frac{1}{q_m K_L} + \frac{1}{q_m C_e} \quad (1)$$

q_e (mg/g) signifies maximum adsorption, C_e (mg/L) denotes the optimum concentration of the metal ion, K_L (L/mg) denotes constant, and q_m (mg/g) is the theoretical optimum adsorption capacity.

2.3.5. Freundlich Model

The Freundlich isotherm (Equation (2)) describes multilayer adsorption mechanisms in which the metal ion interacts with the heterogeneous surface, giving divergent adsorption energy on the entire surface [49].

$$q_e = \frac{1}{n_F} \ln C_e + \ln K_F \quad (2)$$

where q_e = equilibrium adsorption of metal ions onto the functionalized adsorbent, K_F = Freundlich constant, and n_F = intensity of the adsorbents.

2.3.6. Temkin Isotherm Model

Temkin isotherm model (Equation (3)) suggests that the adsorbate/adsorbent interaction indirectly affects the adsorption process [50]. This model only accounts for the

irregular range of metal ion concentrations [51]. The linearized expressions used in this study are shown in Equations (3) and (4).

$$q_e = B\ln A_T + B\ln C_e \quad (3)$$

where

$$B = \frac{RT}{b_T} \quad (4)$$

where T equals temperature (K), R = universal gas constant, b_T is the constant connected to adsorption heat (KJ/mol), and A = constant (L/g).

2.3.7. Dubinin-Radushkevich Isotherm Model (D-R)

The D-R model describes the relationship between the adsorption curve and the surface area of the biosorbents [52]. Additionally, this isotherm model predicts the multilayer interaction using Van Der Waal's force, which is used in the physical adsorption procedure [53]. The Dubinin-R linear equation is generally represented as follows:

$$\ln q_e = \ln q_m - B\varepsilon^2 \quad (5)$$

where B denotes constant, while q_m (mg/g) signifies theoretical equilibrium.

2.3.8. Flory-Huggins Isotherm

Flory-Huggins model gives insight into the extent of surface coverage of the sorbate interactions on the sorbent [54]. The linearized equation used in this study is shown in Equation (6).

$$\ln\left(\frac{\theta}{C_o}\right) = \ln K_{FH} + n\ln(1-\theta) \quad (6)$$

where θ = degree of surface coverage, n = number of sorbates entrapped in the adsorption areas, and K_{FH} are Flory–Huggin's constants ($Lmol^{-1}$).

2.4. Kinetics Study

In this study, pseudo-first-order (PFO), pseudo-second-order (PSO), and intra-particle diffusion models (ID) were employed to investigate the adsorption rates. The linearized expression of the PFO, PSO, and intra-particle diffusion model equations are shown in Equations (7)–(9), respectively [30,31,55,56].

$$\log\,(q_{e,cal} - q_t) = \log\, q_{e,cal} - k_1 t \quad (7)$$

$$\frac{t}{q_t} = \frac{1}{k_2 q_{e,cal}} + \frac{t}{q_{e,cal}} \quad (8)$$

$$q_t = k_3\, t^{0.5} + C \quad (9)$$

where q_t (mg/g)denotes adsorption efficiency in a specific time t (min), K_1 (min^{-1}), K_2 (mg/g min), and K_3 ($g/mg\ min^{-1/2}$) describe the rate constants of the PFO, PSO, and ID models, respectively, and C = intercept.

2.5. Thermodynamic Equilibrium

Thermodynamic equilibrium was estimated to study the process of metal ion uptake, its feasibility, and spontaneity. The following equations were used in the study [57].

$$\Delta G^{\circ} = -\,RT\ln K_C \quad (10)$$

$$\ln K_C = -\left(\frac{\Delta H^\circ}{R}\right) + \left(\frac{\Delta S^\circ}{R}\right) \quad (11)$$

where the values for K_C were estimated using Equation (12)

$$K_C = \frac{q_e}{C_e} \quad (12)$$

where ΔG° = change in standard Gibbs free energy, R is a universal gas constant 8.314 $Jmol^{-1}$ K^{-1}, and T = Temperature, ΔH°, ΔG°, and ΔS° denotes change in enthalpy, free energy, entropy, respectively, and $_{FH}$ = adsorption equilibrium constant.

2.6. Removal Efficiency and Uptake Capacity

The percentage of the metal ions removed and the adsorption capacity of the adsorbents for Pb(II) were estimated using Equations (13) and (14), respectively.

$$\text{Percentage removal efficiency} = \frac{100(C_o - C_e)}{C_o} \quad (13)$$

$$q_e = \frac{(C_o - C_e)V}{m} \quad (14)$$

where C_o = the initial metal ion (mg/L), C_e (mg/L)= equilibrium concentration, q_e (mg/g)= maximum adsorption capacity, V (L) denotes volume, and m (g) = adsorbent mass.

Error Functions

To assess how well the kinetic models fit the experimental data, two error functions were examined. The Hybrid Fractional Error Function (HYBRID) was used to improve the fit of the square of errors function at low concentration levels. The Marquardt's Percent Standard Deviation (MPSD) error function is similar to a geometric mean error distribution that has been adjusted based on the system's degree of freedom [58]. The HYBRID is presented in Equation (15)

$$\text{HYBRID} = \frac{100}{n-p}\sum\left[\frac{\left(q_{e,exp} - q_{e,cal}\right)}{q_{e,exp}}\right]^2 \quad (15)$$

MPSD error function is presented in Equation (16).

$$\text{MPSD} = 100\sqrt{\frac{1}{(n-p)}\sum\left(\frac{q_{e,exp} - q_{e,cal}}{q_{e,exp.}}\right)^2} \quad (16)$$

where $q_{e,exp}$ = experimental adsorption capacity, $q_{e,cal}$ = calculated adsorption capacity, n = number of experimental data points, and p = the number of each parameter.

3. Results and Discussion

3.1. Characterization of Adsorbents

3.1.1. Fourier Transform Infra-Red Spectroscopy (FTIR)

Figure 3A–F illustrate the FTIR spectra of the biosorbents and the functional groups present in the adsorbent before and after the adsorption process. As presented in Figure 3A, the broad peak between 1250–750 cm^{-1} is attributed to the C–O bending vibration of carboxylic groups, alcohol, ketones, and aldehydes [59]. The bending peak at 1543 and 1464 cm^{-1} was due to the C–O bending vibration of carboxylate (–COO–) and the N–H of the amide 1 group [60]. The band between the range of 1700–1733 and 1650 cm^{-1} suggests conjugated carbonyl (C=O) and (C=C). 2063 cm^{-1} denotes carbon triple bond carbon or

CN). The peaks between 2923 and 2852 cm^{-1} range correspond to the stretching vibration of the C–H aliphatic. The broad peak at 3433 cm^{-1} correlates with the stretching vibration of the OH^{-} and N–H groups of the cellulose, hemicellulose, and lignin materials [61]. The oxygen-rich functional groups (–OH), (–C=O), and (–COOH) that account for the binding of the metal ion with the adsorbent are rich in both cellulosic and hemicellulose materials [62].

On activation, there was a sudden disappearance of 1650 cm^{-1} attributed to C=C and the C-O bending vibration of carboxylate (–COO–)in the ethylene glycol modified (E-PA) adsorbent (Figure 3B), as well as observable shifts in the wave numbers of the activated adsorbent before and after adsorption. Some of the observed shifts are 3433 to 3505, 2923 to 2905, 2063 to 2099, 1733 to 1734 and 1464 to 1462 cm^{-1} for E-PA, and 3433 to 3432, 2063 to 2086, and 1543 to 1556 cm^{-1} for I-PA (Figure 3C). The observed shifts in peaks in the FTIR spectra after modification can be attributed to the interactions between functional groups of the adsorbent and the Pb(II) ion. This modification ensured that there were no interferences with undesirable compounds during the adsorption process and increased the pore cavities and surface area of the adsorbent [63].

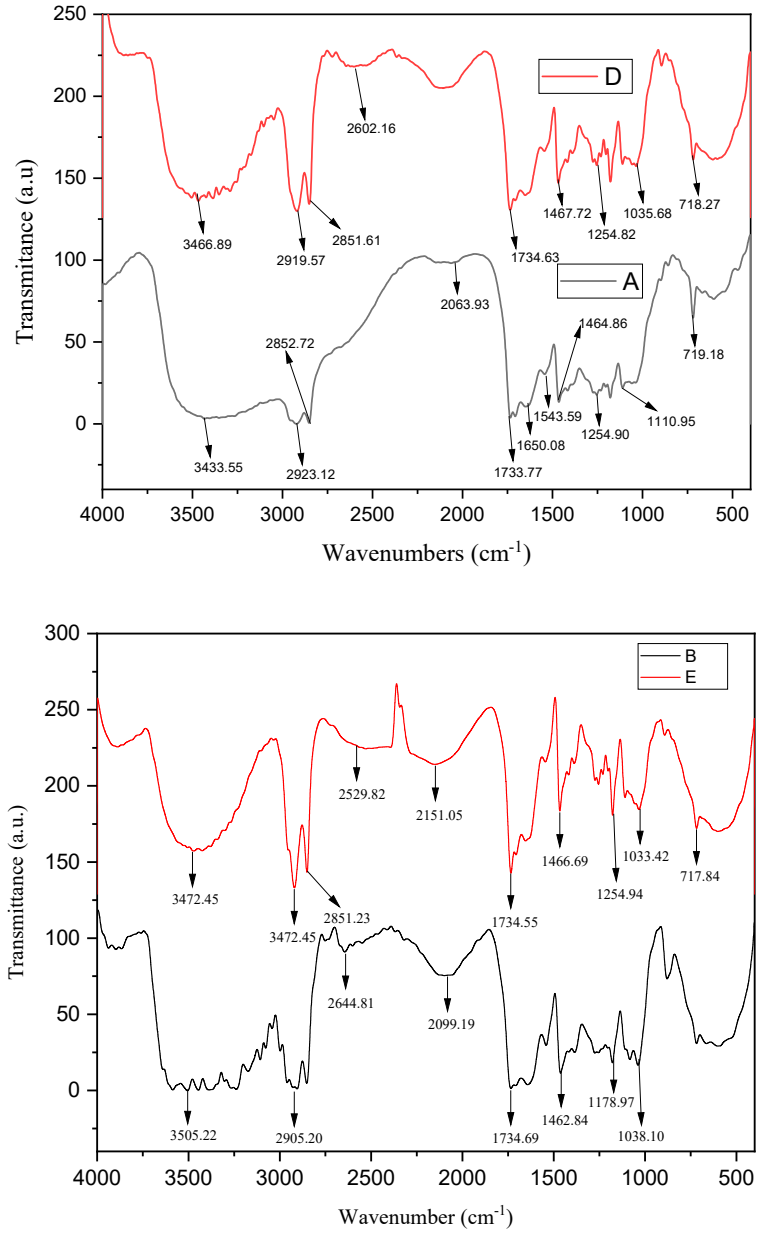

Figure 3. *Cont.*

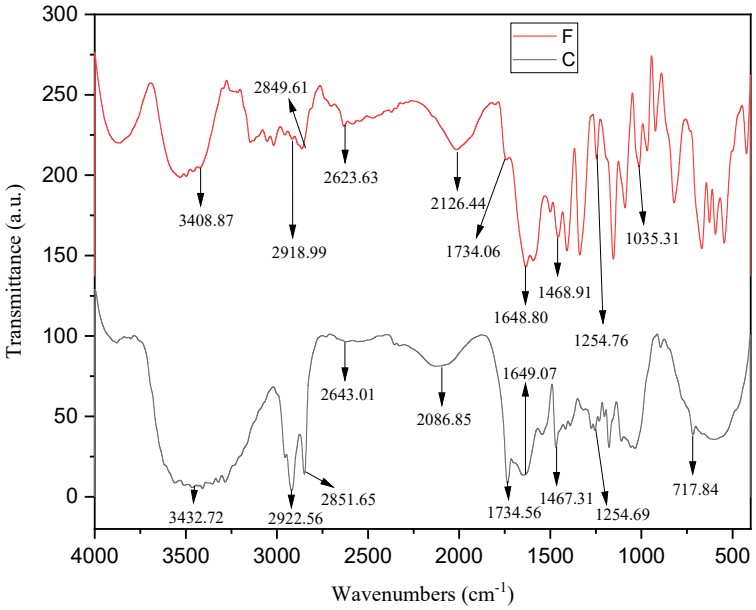

Figure 3. FTIR spectra of P-PA (A), Pretreated E-PA (B), I-PA (C), and spent P-PA (D), spent E-PA (E), spent I-PA (F) of *Pycnanthus angolesis* seed husk.

The spectra of the spent adsorbents confirm the participation of (–OH, –NH, C–O, and C=O) functional groups in the adsorption of Pb(II) ion and changes in the broadband of some peaks after Pb(II) adsorption, indicating the adsorption process of the target metal binding on the sorbent surface [26].

3.1.2. SEM Analysis

The surface morphologies of the adsorbents before modification, after modification, and after adsorption under different magnifications are presented in (Figure 4). The pure adsorbent (see Figure 4A) shows shallow pore structures. However, after modification (Figure 4B,C), the outer surface showed a heterogeneous, rough, uneven display of its surface with sufficient cavities, which will possibly be favorable for the adsorption of Pb(II) ion. The rough, sufficient, and larger cavities observed could be attributed to the impacts of the activation on the sorbent [25].

After adsorption, due to the presence of Pb(II) impurities, the SEM image revealed a homogenous and filled surface (Figure 4E,F) [64]. Similar observations have been reported by other researchers [23,65]. Shafiq et al. [65] developed a biosorbent from *Eucalyptus camdulensis* biochar. Before adsorption, the external EU-biochar surface was rough and had significant pore structures, while after adsorption processes, the adsorbent surface consisted of minute particles and brighter zones.

3.1.3. X-ray Diffraction

The XRD analyses were employed to understand and give insight into the crystal nature of the modified biosorbents. The results obtained for the I-PA and E-PA are shown in Figure 5. E-PA (see Figure 5a) spectra showed five diffraction peaks at 2θ = 25°, 30°, 36°, 44° and 62° attributed to the reflective planes of (110), (111), (121), (200), (311), respectively, while I-PA (see Figure 5b) reveals similar cellulosic diffraction at 2θ = 30°, 35°, 40°, 55.5°, 65.2° corresponding to (110), (111), (121), (200), and (311) planes of reflection, respectively. The sharp peaks obtained in these diffractions suggest a distinct alignment of a perfect crystalline structure [66]. Akpomie and Conradie [55] obtained similar cellulose diffraction peaks for a natural organic-silver nanocomposite for oil removal in water. The sharp peaks obtained in these spectra could be attributed to the influence of the chemical modification on *Pycnanthus angolesis* seed husk.

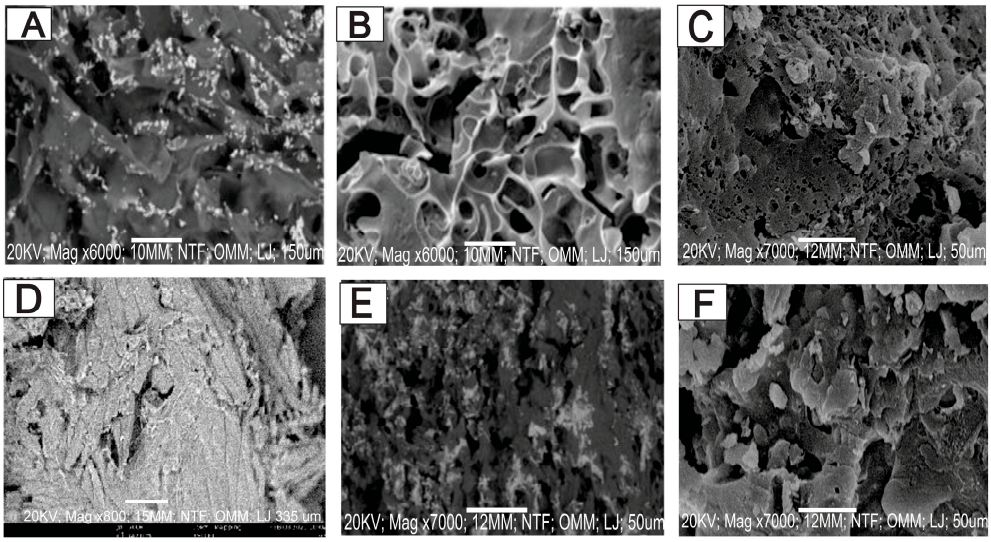

Figure 4. SEM images of (P-PA (**A**), E-PA (**B**), I-PA (**C**), spent P-PA (**D**), spent E-PA (**E**), spent I-PA (**F**)).

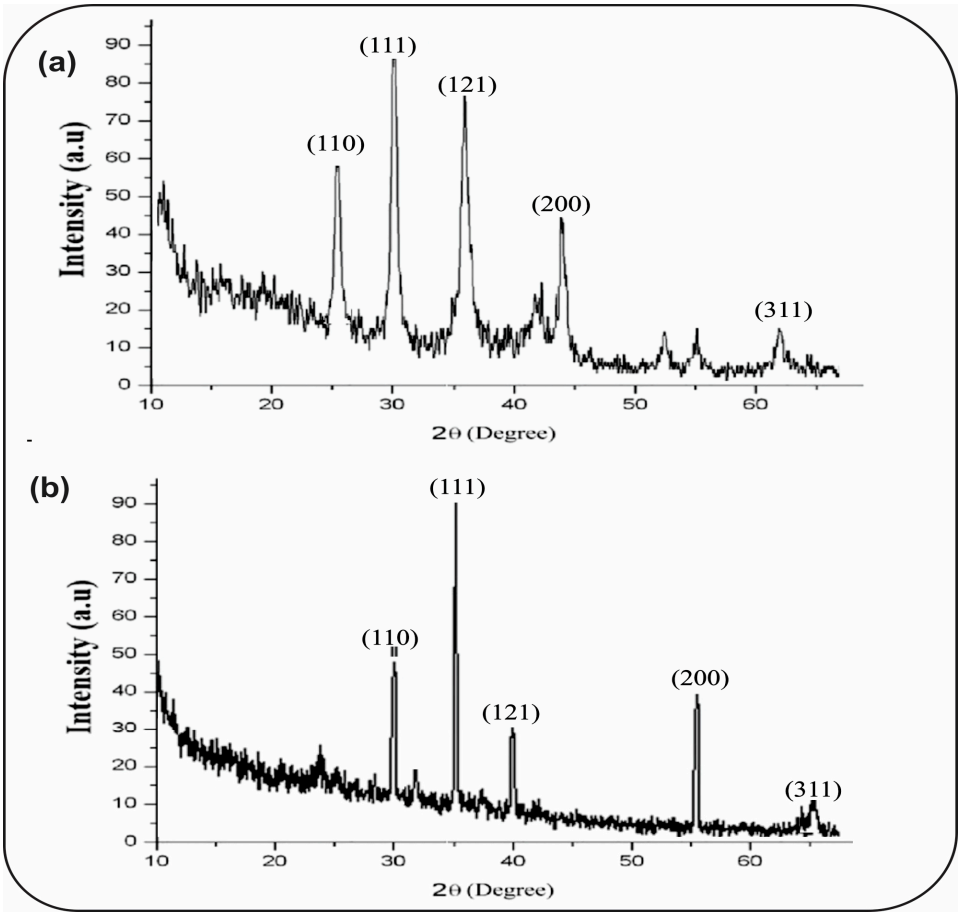

Figure 5. XRD spectra of E-PA (**a**) and I-PA (**b**) modified *Pycnanthus angolensis* seed husk.

3.1.4. Brunauer-Emmett-Teller (BET) Analysis

The physicochemical features of the pure *Pycnanthus angolesis* seed husk (P-PA) and the modified (E-PA and I-PA) were presented in Table 2. From the data generated, the surface area and pore volume of the pure biosorbent are 65.200 m^2/g and 0.055 cm^3/g, respectively. The surface area of the ethylene-glycol-activated adsorbent is 66.400 m^2/g,

with a pore volume of 0.6355 cm^3/g, while 60.500 m^2/g and 0.6355 cm^3/g were obtained for the surface area and pore volume of the Iso-butanol activated adsorbent, respectively.

Table 2. Physiochemical features of pure (P-PA) and modified (E-PA and I-PA) *Pycnanthus angolensis* seed husk adsorbent.

Adsorbent Type	Surface Area (m^2/g)	Pore Volume (cm^3/g)	Pore Diameter (Å)
P-PA	65.200	0.605 24.540	24.540
E-PA	66.400	0.635	28.340
I-PA	60.500	0.635	30.340

The surface area obtained for the iso-butanol and ethylene glycol adsorbents is higher than some of the previously reported works, such as the acid-modified onion skin at 10.62 m^2/g [67], garlic waste at 5.62 m^2/g [68], and fennel seed at 3.668 m^2/g [16]. Comparatively, the activated adsorbents showed higher pore sizes than the pure adsorbent. The high pore size obtained could be attributed to the dissolution of hemicelluloses and pectin from the cell wall of the sorbent [69]. The high surface area and pore diameter obtained indicate an abundant adsorption site on the adsorbent surfaces [70]. Table (see Table 2) shows an increase in pore size, pore volume, and surface area of the treated adsorbent compared to the pure sample (P-PA), suggesting that the ethylene glycol and iso-butanol (E-PA and I-PA) activated adsorbent could be more efficient in the adsorption process.

3.2. Thermal Stability

Figure 6 shows the thermal stability of the pure ethylene glycol and iso-butanol-modified *Pycnanthus angolesis* seed husk (P-PA, E-PA, and I-PA). The result showed that the samples were stable up to 500 °C with three stages of degradation. An initial mass loss of −0.035 mg was observed in all the samples below 275, 255, and 270 °C for the P-PA, E-PA, and I-PA, respectively.

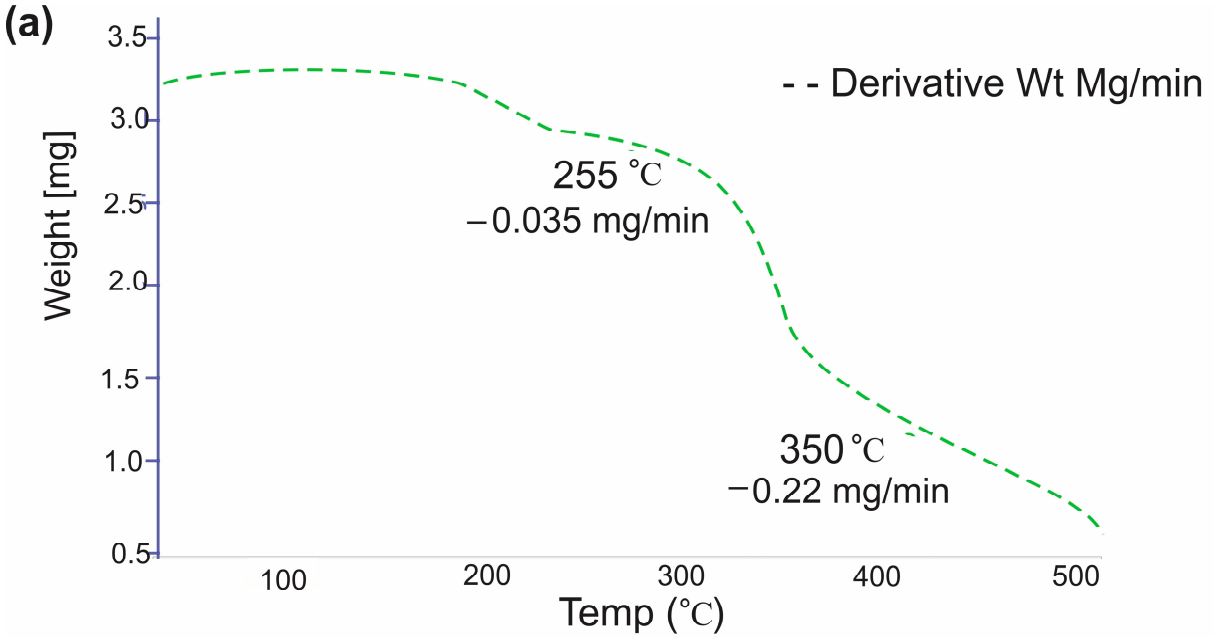

Figure 6. *Cont.*

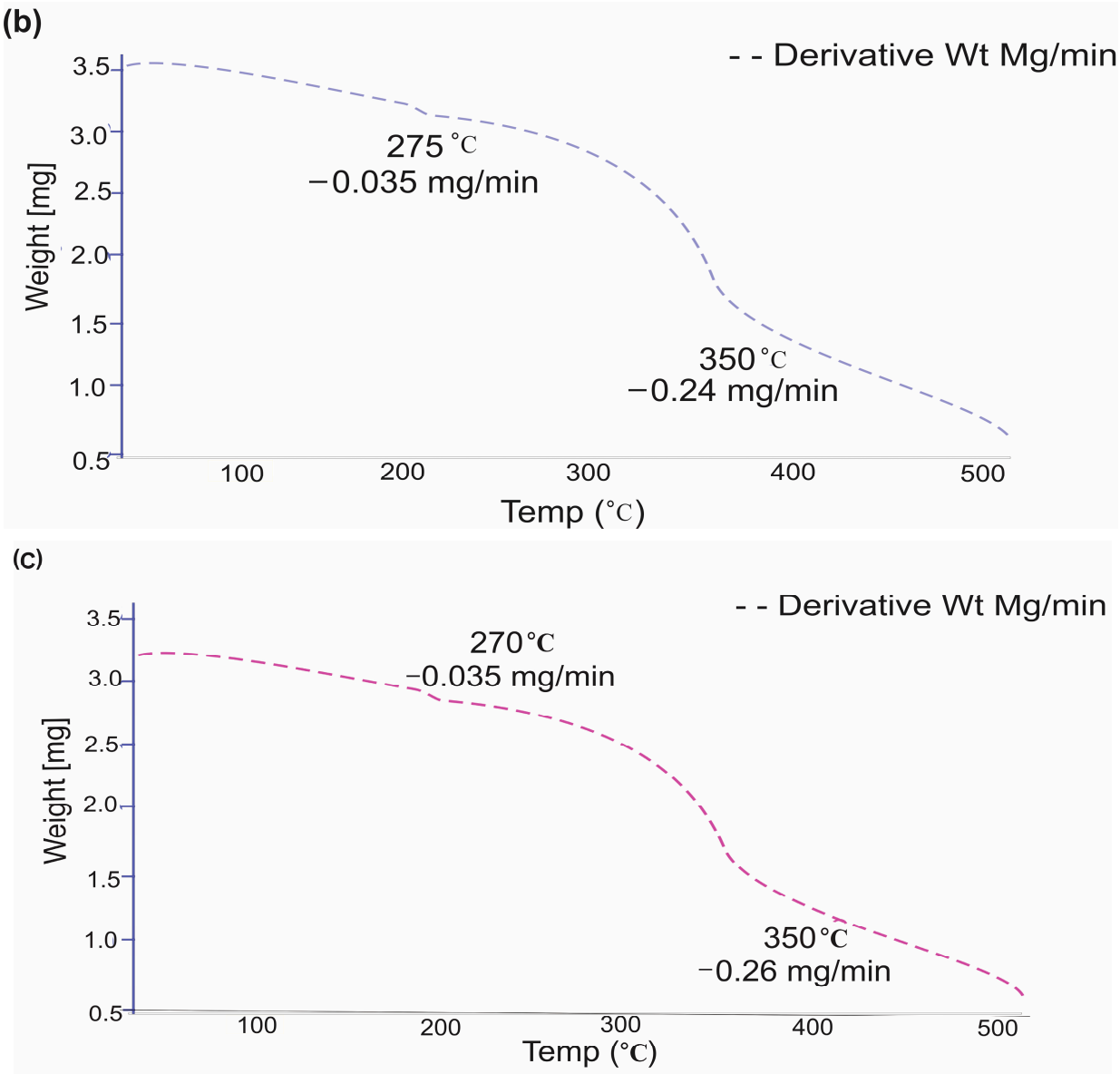

Figure 6. TGA thermogram of P-PA (**a**), E-PA (**b**) and I-PA (**c**).

This initial weight loss is linked to the loss of water from the adsorbents. Another mass loss of 0.24, 0.22, and 0.26 mg was observed on the TGA curve from 255 to 350 °C for P-PA, E-PA, and I-PA, respectively, due to the breakdown of hemicellulose and cellulose and the subsequent formation of a carbonaceous residue, which decomposes until it reaches 500 °C for all the adsorbent. This observation agrees with the reports of Eze et al. [23] on the TGA/DTA analysis of *Terminalia mantaly* seed husk biosorbent for the sequestration of ions from an aqueous solution.

3.2.1. Effect of pH

In adsorption studies, the pH study is an important parameter because it affects both the oxidation state of the contaminants in the aqueous system and the surface property of the adsorbent [71]. Its impact in this study was determined at pH 2, 4, 6, 8, and 10 on 10 mg/L at 298 K, as presented in Figure 7 for the P-PA and E-PA and I-PA, respectively. From the graph, there was an observable rapid increase in Pb(II) ion adsorption with an increase in pH value from 2 to 4 in the pure adsorbent before attaining equilibrium at pH 6 (see Figure 7). A spontaneous increase at lower pH was also observed for the modified adsorbents up to pH 6 (Figure 7).

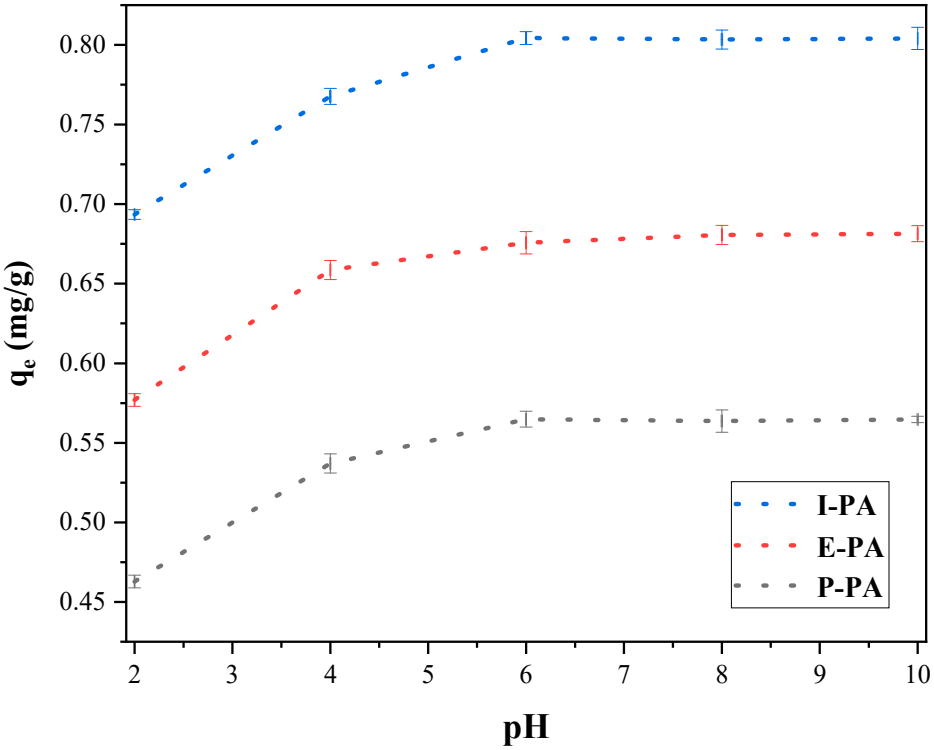

Figure 7. Effect of pH on Pb(II) onto P-PA, E-PA, and I-PA at 10 mg/L at 298 K reaction condition.

This is due to the activation of the surface functional groups, a decrease in hydrogen ion concentration, and electrostatic desirability, which promote metal ion adsorption [72]. The optimum adsorption efficiency of Pb(II) ion was achieved at pH 6 for all the adsorbents. At this point, the adsorption of Pb(II) ions remained constant. This is because, at a higher pH, the adsorption efficiency decreases as a result of the formation of soluble hydroxyl complexes and insoluble hydroxide precipitation [73]. Similar observations were also reported by Wang et al. [74] and Radha et al. [75].

3.2.2. Effect of Contact Time

For the pure adsorbent (Figure 8), the adsorption occurs relatively rapidly within the first 120 min and remains constant after 180 min. I-PA (Figure 8) showed rapid adsorption until maximum adsorption removal was attained at 180 min and decreased gradually after 200 min, while E-PA increased gradually from 50 to 120 min before attaining equilibrium at 180 min. The rapid increase in adsorption could be attributed to sufficient adsorption sites, making Pb(II) interact easily with the site [76]. In this study, the maximum adsorption time obtained was faster than in the study of Radha et al. [75], which used a chitosan-derived copolymeric blend for Pb(II) ion and Cd^{2+} ion removal.

This result is corroborated using the SEM image (see Figure 4), which shows that after modification, the outer surface showed a heterogeneous, rough, uneven display of its surface with sufficient cavities, which will possibly be favorable for the uptake of Pb(II) ion [77]. After equilibrium was achieved, further increases in time resulted in no significant change in the Pb(II) adsorption, showing that the binding sites are already saturated for the adsorption of Pb(II) ion [4]. Similar results were observed for the uptake of Pb(II) ion using biosorbent derived from the endocarp waste of Gayo coffee [27].

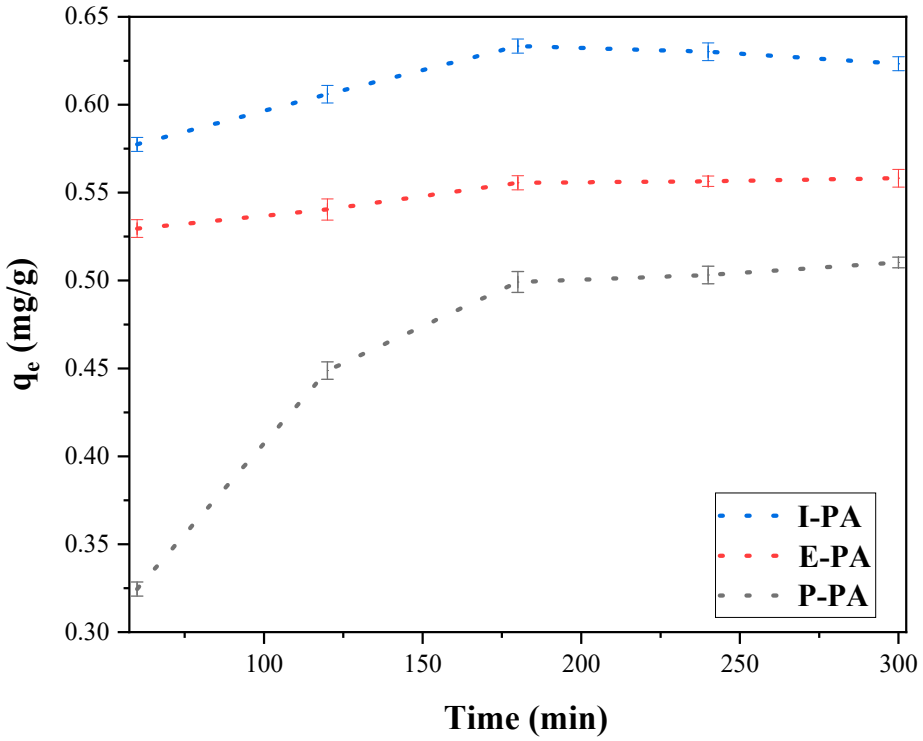

Figure 8. Effect of contact time on Pb(II) onto P-PA, E-PA, and I-PA.

3.2.3. Effect of Initial Metal Concentration

Figure 9 illustrates the impacts of metal ion concentration on the adsorption capacity of the prepared adsorbents for the uptake of lead. The sequestration of Pb(II) ion onto the P-PA, E-PA, and I-PA increased rapidly with an increase in the initial concentration of Pb(II) ion in the aqueous system. The reason is that at the initial adsorption stage, there is a higher usage of the active sites or enormous availability of unused active sites on the adsorbents [78]. Previous studies have reported a similar rapid increase in adsorption capacity with an increase in initial metal concentration [79].

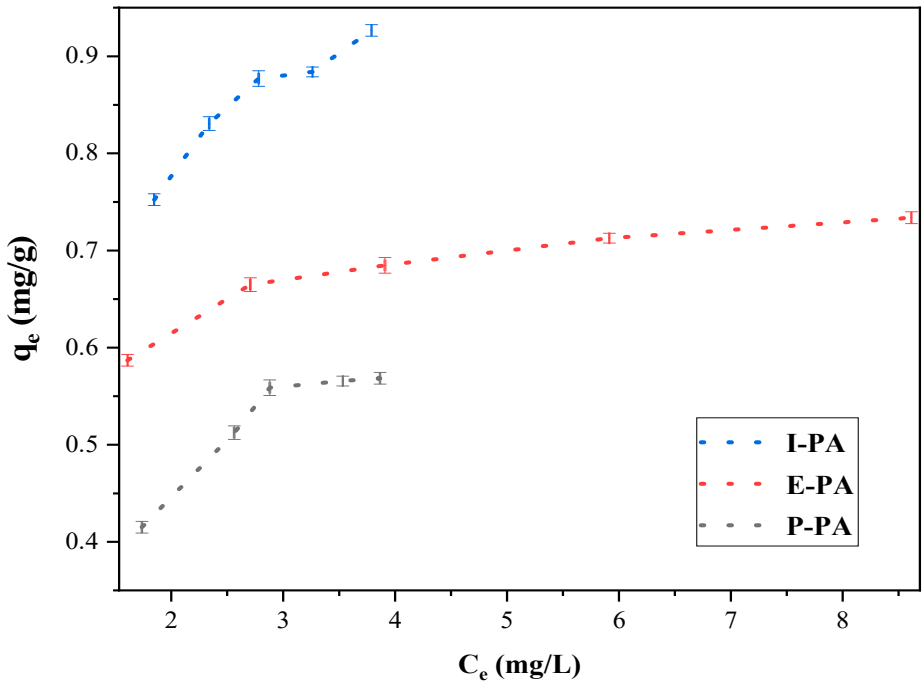

Figure 9. Effect of concentration on Pb(II) onto P-PA, E-PA, and I-PA.

3.3. Isotherm Studies

The isotherm models give insight into the adsorption mechanism, adsorbent-adsorbate interaction, and adsorbent materials [80]. The coefficient of regression (R^2) obtained from the plot of each model was used to select the isotherm model that correlates better with the adsorption of Pb(II). The parameters and estimated adsorption isotherm are shown in Table 3.

Table 3. Estimated values obtained for different Parameters of the isotherm models.

Isotherm Model	Parameters	P-PA	E-PA	I-PA
Langmuir	q_m (mg/g)	0.714	0.581	0.523
	K_L (L/g)	0.866	3.685	−20.141
	R_L	0.025	0.0059	−0.011
	R^2	0.985	0.992	0.987
Freundlich	K_F ((mg/g)/(mg/L) n)	0.483	0.443	0.414
	n	14.854	7.622	5.328
	R^2	0.628	0.674	0.749
Temkin	A_t (L/g)	473.212	1.387	3.301
	B	0.073	0.161	0.197
	b_t (kJ/mol)	34.047	15.415	12.601
	R^2	0.788	0.733	0.704
D-R	q_m	0.803	0.785	0.8074
	E	−30.30	−36.523	−25.649
	R^2	0.905	0.551	0.805
Florry Huggins	K_{FH}	0.014	0.001	0.002
	n_{FH}	−1.734	−3.034	−2.677
	R^2	0.410	0.733	0.501

Langmuir Isotherm model suggests a monolayer adsorption mechanism and the possible formation of a homogenous surface on the sorbent. The regression coefficients (R^2 = 0.985, 0.992, and 0.987) obtained from this model for P-PA, E-PA, and I-PA adsorbents, respectively, are higher than the ones obtained from other models, suggesting a perfect description of the experimental data. The perfect fits obtained suggest that the adsorption surfaces are homogenous, and the adsorption process follows a monolayer adsorption mechanism [81]. The maximum adsorption capacities (q_m) estimated were 0.714, 0.581, and 0.523 mg/g for the P-PA, E-PA, and I-PA, respectively. The Freundlich isotherm suggests a multilayer adsorption mechanism and a likely heterogeneous adsorption surface [55]. The values of the correlation coefficient (R^2 = 0.628, 0.674, and 0.749) obtained for the pure adsorbent and both modified adsorbents are lower than those obtained in the Langmuir isotherm. This implies that the Freundlich isotherm does not correlate best with the removal of Pb(II) ion onto the sorbents. However, the n values obtained for the adsorption study are <10, indicating a favorable removal of Pb(II) ions by the adsorbents [56]. Temkin models give insight into adsorbent and adsorbate interactions. The lower R^2 values (0.788, 0.733, and 0.704) obtained are lower than the ones obtained for the Langmuir model and thus do not correlate better with the uptake of Pb(II) ion onto the adsorbents. The Dubinin–Radushkevich isotherm is used to evaluate the nature of the adsorption process (a physical or chemical reaction) [82]. The lower regression coefficient values (R^2 = 0.905, 0.551, and 0.805) and (R^2 = 0.410, 0.733, and 0.501) obtained for the Dubinin–Radushkevich Isotherm and Flory Huggins models for P-PA, E-PA, and I-PA, respectively, denote that these models do not correlate best in describing the process of Pb(II) ion removal.

3.4. Kinetics Studies

The kinetic data obtained from the studies of PFO, PSO, and ID were used to study the adsorption mechanism of the Pb(II) ion on the adsorbents. The estimated kinetic parameters are presented in Table 3. The comparison of the kinetic models shows that

PFO best describes the kinetic adsorption of Pb(II) ion onto the adsorbents than PSO due to the degree of closeness between the $q_{e,Exp}$ and the $q_{e,cal}$ suggesting a physical adsorption process (formation of a weaker bond), which could be the reason for the lower adsorption capacity.

The lesser values obtained in HYBRID and MPSD error function analysis for the PFO (Table 4) also supported this observation. The intra-particle plot for pure and Isobutanol *Pycnanthus angolensis* seed husk did not pass through the origin, suggesting that film and intra-article diffusion simultaneously controlled the rate-limiting step [83]. This observation is similar to the adsorption of Pb(II) ions onto naturally aged and virgin microporous materials [84].

Table 4. Kinetic parameters for the uptake of Pb(II) ion on the pure and modified adsorbents.

Kinetic Models	Parameter	P-PA	E-PA	I-PA
$q_{e,Exp}$		0.526	0.534	0.565
Pseudo-first-order				
	K_1 (min^{-1})	−0.007	−0.008	−0.002
	$q_{e,cal}$ (mg/g)	0.344	0.387	0.153
	R^2	0.763	0.897	0.885
HYBRID		5.133	3.23	17.79
MPSD		36.172	32.201	49.337
Pseudo-second-order				
	$q_{e,cal}$ (mg/g)	1.139	1.098	2.517
	K_2 (L/mg min)	−0.023	−0.021	0.022
	h (mg/L min)	−0.029	−0.024	0.142
	R^2	0.942	0.954	0.972
HYBRID		34.332	29.651	397.862
MPSD		58.137	56.302	107.238
Intra-particle diffusion				
	K_3 (mg/g $min^{-1/2}$)	0.125	0.340	0.094
	C	0.555	−1.829	0.952
	R^2	0.823	0.861	0.719

3.5. Thermodynamic Studies

Table 5 lists the estimated thermodynamic parameters for the adsorption of Pb(II) ions onto the P-PA, E-PA, and I-PA. The equations used in evaluating these parameters were established (see Equations (10) and (11)). The ΔG° values for the sequestration of Pb(II) ion unto the adsorbents were negative for all adsorbents, showing that the adsorption process was spontaneous (i.e., occurred without the input of external energy).

Table 5. Calculated values of Thermodynamic parameters.

Adsorbents	T (K)	ΔG° (kJ/mol)	ΔH° (kJ/mol)	ΔS° (J/mol K)
P-PA	313	−8.83	−33.91	−81.91
	323	−6.06		
	333	−7.32		
E-PA	313	−1.04	32.82	78.48
	323	−5.90		
	333	−7.47		
I-PA	313	−8.56	73.85	206.60
	323	−8.08		
	333	−4.45		

For E-PA, it was observed that Gibbs free energy decreased as the temperature increased, indicating that the removal efficiency was enhanced at high temperatures [85]. The negative value of ΔH° obtained for the pure adsorbent depicts exothermic adsorption, while upon impregnation, the endothermic nature of the adsorption process was indicated by the positive values of ΔH° [86]. In addition, the increased random interaction observed during the adsorption process of the Pb(II) ion onto the modified adsorbents

was indicated by the positive ΔS° against the negative value ΔS° obtained for the pure adsorbents [87]. Ghanim et al. [79] observed a similar result using acid-modified poultry litter-derived hydrochar.

3.6. Adsorption Mechanism

The determination of the adsorption mechanism is of considerable significance in understanding the adsorption process. This process relies on various factors, including the morphology and functional groups that exist on the surface of the adsorbent, as well as the size and charge characteristics of the contaminants [16]. *Pycnanthus angolensis* seed husks consist primarily of lignocellulosic materials, which consist of hemicellulose, cellulose, and lignin. Lignocellulosic materials possess a significant abundance of oxygen-rich functional groups, including hydroxyl (–OH), carbonyl (–CO), and carboxyl (–COOH), which makes them very suitable for adsorption processes [88]. The mechanism that controls the adsorption process is illustrated in Figure 10. To assess the mechanism of adsorption that controls the sequestration of Pb(II) from aqueous solution unto the *Pycnanthus angolensis* seed husk, spectroscopic techniques (SEM and FTIR) were employed. Deduction from the SEM analysis showed that the adsorption of Pb(II) unto the surface of the adsorbents was necessitated due to the large pore structures observed, which served as a binding site for Pb(II) and were further corroborated by the assessment of the kinetic model that suggested physisorption. In addition, the shifts and disappearance of the broad band observed in the FTIR spectra (see Figure 3B,C) suggest the likelihood of a chemical adsorption mechanism. The charged ion on some of the functional groups (OH, N–H, COOH, C=O) identified using the FTIR on the adsorbents may interact with the ion of the sorbate via the interaction between the negatively charged oxygen and the positively charged metal ion (electrostatic interaction), ion exchange, and the formation of a complex with the oxygen-carrying group on the adsorbents. Therefore, it is assumed that, with the functional groups present on the adsorbent's surface and the presence of hydrogen bonding and cation interaction, the removal of Pb(II) from the aqueous solution is probable. This observation is similar to the report of Mabungela et al. [16] on the adsorption of Pb(II) onto fennel seeds and Wang et al. [74] on the Pb(II) adsorption using pectin/activated carbon-based porous microspheres.

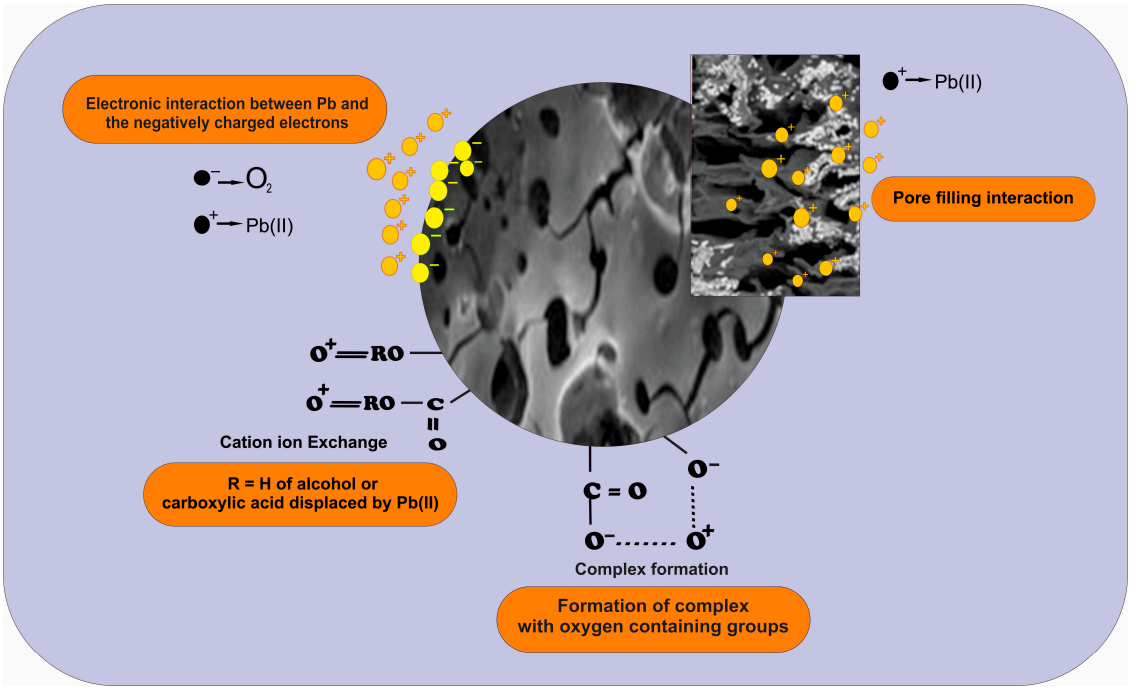

Figure 10. Schematic mechanism of Pb(II) adsorption onto pure and modified *Pycnanthus angolensis* seed husk.

3.7. Comparing the Performance of Pycnanthus angolensis Seed Husk with Other Adsorbents

The results of this study were compared to those of previous studies that used different adsorbents to study the adsorption of Pb(II). A comparison of these results is presented in Table 6. Pretreated *Pycnanthus angolensis* showed lower adsorption capacity compared to some of the adsorbents previously reported. However, despite the lower adsorption capacity observed, it showed a higher percentage removal efficiency of 96.75, 96.44, and 95.91% compared to most biosorbents previously reported (Table 5). Therefore, it is still recommended for the treatment of wastewater and for the use of other forms of modifying agents (acid, base, or thermal) to enhance its absorption capacity.

Table 6. Comparison of properties of *Pycnanthus angolensis* seed husk with other adsorbents used for the adsorption of Pb(II).

Biosorbent	q_m (mg/g)	Isotherm Model	Optimal pH	% Removal Efficiency	Reference
Chemically pretreated *Pycnanthus angolensis* Seed Husk	0.714	Langmuir	6	96.75	This study
Acid-treated fennel seed	18.79	Langmuir	8	-	[16]
Banana peel	2.18	Langmuir	5	-	[89]
Bagasse fly ash	2.50	Langmuir	5	95.00	[90]
Black sapote seeds	5.50	Langmuir	9	96.60	[91]
Melocanna baccifera (Poaceae)	10.66	Langmuir	6	81.69	[92]
Orange Peel Cellulose	50.10	Langmuir	4	98.33	[29]
Dyed shells of groundnut	0.106	Langmuir	-	-	[93]
Soya bean	0.72	Langmuir	4	70.42	[94]

3.8. Research Implications for Wastewater Treatment and Contributions to Sustainability

The need for proficient wastewater treatment methods has been driven by the dearth of safe drinking water as well as other environmental consequences. Adsorption techniques are gaining popularity as a practical method for detoxifying contaminated water. Despite a wide range of adsorbents being discussed in the literature, biosorption is a viable alternative method for eliminating contaminants from water [95]. It has a number of benefits, including ease of use, good adsorption capacity, high recoverability, and the ability to be modified [96]. A growing number of biosorbents have been developed and enhanced using environmentally friendly, secure, and cost-effective processes adhering to the ideals of sustainable chemistry [97]. Biosorbents offer interesting and intriguing properties for the removal of contaminants. Additionally, the sorbents exhibit excellent adsorption qualities and capacities following a variety of activations that enhance the rate of the adsorption process. In light of these, the use of modified *Pycnanthus angolensis* seed husk in the sequestration of Pb(II) from wastewater, as well as its kinetics, isotherm, and mechanism of adsorption, were explored.

This research paper holds significant implications for sustainability in the context of wastewater treatment and environmental protection. The results demonstrated the potential of the use of modified *Pycnanthus angolensis* seed husk for applications in real-life scenarios for the regeneration of biosorbents. Below are some of the key ways in which this research aligns with sustainability principles:

Pollution mitigation: This research addresses the pressing issue of lead pollution in water, a matter of significant environmental concern in recent times. Lead contamination has detrimental effects on human health and aquatic ecosystems. By developing an effective method for lead removal from wastewater, this research contributes to reducing water pollution and protecting the environment.

Resource efficiency: The utilization of the *Pycnanthus angolensis* seed husk as a natural adsorbent for lead ion removal represents a sustainable approach, as it would potentially reduce the reliance on synthetic and non-renewable materials in metal removal from

aqueous solutions, such as in wastewater treatment process. This method thereby promotes resource efficiency and minimizes the ecological footprint of conventional treatments.

Renewable and biodegradable material: *Pycnanthus angolensis* seed husk is a renewable and biodegradable resource, offering the choice for commitment to sustainable practices of using environmentally friendly alternatives to synthetic adsorbents. Studies have reported that synthetic adsorbents often pose disposal challenges and environmental harm.

Low-cost solution: The findings of this research offer a cost-effective solution for lead removal from aqueous media and for wastewater treatment, especially for many resource-constrained developing countries and regions. The cost-effectiveness of the *Pycnanthus angolensis* seed husk method enhances its applicability and aligns with sustainability goals of affordability and accessibility.

Reduced energy consumption: The proposed lead adsorption method also contributes to sustainability, as it requires less energy compared to traditional treatment processes. This reduction in energy consumption will not only lower the operational costs but also reduce the carbon footprint associated with wastewater treatment.

Social and environmental impact: The potential positive impacts of adopting this method on local communities and ecosystems cannot be overstated. As more lead contamination cases are addressed in affected areas, the research would help in improving the quality of life of residents and wildlife.

Regulatory compliance: The present research complies with environmental regulations and standards pertaining to wastewater quality. This alignment with established standards underscores commitment to responsible and sustainable research practices.

Long-term benefits: The *Pycnanthus angolensis* seed husk method offers the prospect of long-term sustainability by utilizing a renewable resource and promoting environmentally responsible practices in wastewater treatment. The potential for lasting benefits is central to the sustainability of the proposed approach.

In summary, the research findings have indicated that modified *Pycnanthus angolensis* seed husk can be used to remove Pb(II) from aqueous solutions such as wastewater. This research paper significantly contributes to the needed remediation strategies towards achieving the Sustainable Development Goal (SDG) of ensuring access to clean, safe water and promoting sustainable wastewater treatment practices and water management.

4. Conclusions

In conclusion, the pure adsorbent was successfully modified using ethylene glycol (E-PA) and iso-butanol (I-PA) in order to enhance its adsorption capacity. The FTIR spectra confirm the participation of OH, –NH, C–O, C=O, and C–H functional groups in the uptake of Pb(II) ion and shifts in the broadband of some peaks after Pb(II) ion removal, indicating effective binding of the target metal on the sorbent surface. XRD confirms the influence of the modification on the *Pycnanthus angolesis* seed husk. SEM images of modified adsorbents (E-PA and I-PA) under different magnifications exhibited abundant cracked surfaces, enhanced pore structures, and cavities that can aid in the entrapment of Pb(II) ion compared to the pure adsorbent (P-PA). This result is corroborated by the higher pore size recorded for the E-PA and I-PA compared to the pure adsorbent (P-PA) in BET analysis. TGA revealed that the samples recorded three steps of degradation and were stable up to 500 °C. The linear plot of the isotherm and kinetic models shows that the uptake of Pb(II) ion on the adsorbents correlates better with the Langmuir model, which indicates a monolayer adsorption mechanism and possible formation of a homogenous surface of the sorbent. The kinetics of Pb(II) ion uptake fit best with the pseudo-first-order model and were corroborated by the relatively lower values estimated in the error function for all adsorbents. Thermodynamics revealed a spontaneous and endothermic adsorption process. At the same time, the adsorption mechanism revealed that the uptake of Pb(II) onto the P-PA, E-PA, and I-PA mainly involves electrostatic interaction, surface complexation, physical adsorption, and ionic exchange. In addition, the maximum adsorption efficiency was attained at 180 min at pH 6, while the adsorption increases as the concentration increases

for all adsorbents. The result demonstrated the potential of the use of *Pycnanthus angolensis* seed husk for applications in real-life scenarios for the regeneration of biosorbents. The use of *Pycnanthus angolensis* seed husk significantly contributes to the needed remediation strategies to further the Sustainable Development Goal (SDG) of ensuring access to clean water and promoting sustainable water management.

Author Contributions: A.L.E.: conceptualization, experiments, H.O.A. and J.C.E.: manuscript writing, data analysis, I.A.U.: AAS, FTIR Interpretation, assistance, and proofreading. S.I.E.: data analysis, proofreading. V.S.A.: resources, data analysis, reviewing. K.G.A.: Literature Writing and XRD, TGA Interpretation. All authors contributed to the revisions of the manuscript and approved it for publication. All authors have read and agreed to the published version of the manuscript.

Funding: The authors did not receive any funding.

Institutional Review Board Statement: Not applicable.

Informed Consent Statement: No human or other animals were used in the study.

Data Availability Statement: All data generated or analyzed are available within the manuscript.

Conflicts of Interest: The authors declare that there is no conflict of interest.

References

1. Tsvetanova, L.; Barbov, B.; Rusew, R.; Delcheva, Z.; Shivachev, B. Equilibrium Isotherms and Kinetic Effects during the Adsorption of Pb(II) on Titanosilicates Compared with Natural Zeolite Clinoptilolite. *Water* **2022**, *14*, 2152. [CrossRef]
2. Guo, Z.; Zhan, R.; Shi, Y.; Zhu, D.; Pan, J.; Chao, Y.; Wang, Y.; Wang, J. Innovative and Green Utilization of Zinc-Bearing Dust by Hydrogen Reduction: Recovery of Zinc and Lead, and Synergetic Preparation of Fe/C Micro-Electrolysis Materials. *Chem. Eng. J.* **2023**, *456*, 141157. [CrossRef]
3. Li, H.; Zhao, S.; Zhang, W.; Du, H.; Yang, X.; Peng, Y.; Han, D.; Wang, B.; Li, Z. Efficient Esterification over Hierarchical Zr-Beta Zeolite Synthesized via Liquid-State Ion-Exchange Strategy. *Fuel* **2023**, *342*, 127786. [CrossRef]
4. Adebisi, E.U.; Adebisi, A.A.; Okechukwu, V.U.; Omokpariola, D.O.; Umeh, T.C. Adsorption potential of Lead and Nickel ions by *Chrysophyllum albidum* G.Don (African Star Apple) seed shells. *World Sci. News* **2022**, *166*, 132–145.
5. Liu, W.; Zheng, J.; Ou, X.; Liu, X.; Song, Y.; Tian, C.; Rong, W.; Shi, Z.; Dang, Z.; Lin, Z. Effective Extraction of Cr(VI) from Hazardous Gypsum Sludge via Controlling the Phase Transformation and Chromium Species. *Environ. Sci. Technol.* **2018**, *52*, 13336–13342. [CrossRef] [PubMed]
6. Hu, F.; Qiu, L.; Xiang, Y.; Wei, S.; Sun, H.; Hu, H.; Weng, X.; Mao, L.; Ming, Z. Spatial Network and Driving Factors of Low-Carbon Patent Applications in China from a Public Health Perspective. *Front. Public Health* **2023**, *11*, 1121860. [CrossRef]
7. Zhang, N.; Lu, D.; Sheng, H.; Xia, J.; Kan, P.; Yao, Z.; Chen, H.; Li, G.; Zhu, D.Z.; Liu, H. Constructed Wetlands as Hotspots of Antibiotic Resistance Genes and Pathogens: Evidence from Metagenomic Analysis in Chinese Rural Areas. *J. Hazard. Mater.* **2023**, *447*, 130778. [CrossRef]
8. Li, Y.; Li, Y.; Shan, Y.; Tong, H.; Zhao, J. Effect of Magnesium Ions on the Mechanical Properties of Soil Reinforced by Microbially Induced Carbonate Precipitation. *J. Mater. Civ. Eng.* **2023**, *35*, 04023413. [CrossRef]
9. Mao, S.-X.; Song, J.; Zhu, W.; Ji, M.; Pang, J.; Dang, D.-B.; Pang, J. Heterogeneous Oxidative Desulfurization of Fuels Using Amphiphilic Mesoporous Phosphomolybdate-Based Poly(Ionic Liquid) over a Wide Temperature Range. *Fuel* **2023**, *352*, 128982. [CrossRef]
10. Sun, X.; Chen, Z.; Sun, Z.; Wu, S.; Guo, K.; Dong, Z.; Peng, Y. High-Efficiency Utilization of Waste Shield Slurry: A Geopolymeric Flocculation-Filtration-Solidification Method. *Constr. Build. Mater.* **2023**, *387*, 131569. [CrossRef]
11. Zhao, Y.; Li, Q.; Cui, Q.; Ni, S.-Q. Nitrogen Recovery through Fermentative Dissimilatory Nitrate Reduction to Ammonium (DNRA): Carbon Source Comparison and Metabolic Pathway. *Chem. Eng. J.* **2022**, *441*, 135938. [CrossRef]
12. Hayeeye, F.; Qian, Y.; Sattar, M.; Chinpa, W.; Sirichote, O. Adsorption of Pb^{2+} Ions from Aqueous Solutions by Gelatin/Activated Carbon Composite Bead Form. *Adsorpt. Sci. Technol.* **2017**, *36*, 355–371. [CrossRef]
13. Wang, Z.; Chen, C.; Liu, H.; Hrynshpan, D.; Savitskaya, T.; Chen, J.; Chen, J. Enhanced Denitrification Performance of Alcaligenes Sp. TB by Pd Stimulating to Produce Membrane Adaptation Mechanism Coupled with Nanoscale Zero-Valent Iron. *Sci. Total Environ.* **2020**, *708*, 135063. [CrossRef]
14. Zheng, Y.; Liu, Y.; Guo, X.; Chen, Z.; Zhang, W.; Wang, Y.; Tang, X.; Zhang, Y.; Zhao, Y. Sulfur-Doped g-C3N4/RGO Porous Nanosheets for Highly Efficient Photocatalytic Degradation of Refractory Contaminants. *J. Mater. Sci. Technol.* **2020**, *41*, 117–126. [CrossRef]
15. Rind, I.K.; Sarı, A.; Tuzen, M.; Lanjwani, M.F.; Karaman, I.; Saleh, T.A. Influential biosorption of lead from aquatic solution using Escherichia coli/carbon nanofibers. *Environ. Nanotechnol. Monit. Manag.* **2023**, *19*, 100776. [CrossRef]
16. Mabungela, N.; Shooto, N.D.; Mtunzi, F.M.; Naidoo, E.B. The Adsorption of Copper, Lead Metal Ions, and Methylene Blue Dye from Aqueous Solution by Pure and Treated Fennel Seeds. *Adsorpt. Sci. Technol.* **2022**, *2022*, 5787690. [CrossRef]

17. Bai, B.; Rao, D.R.V.P.; Chang, T.; Guo, Z. A Nonlinear Attachment-Detachment Model with Adsorption Hysteresis for Suspension-Colloidal Transport in Porous Media. *J. Hydrol.* **2019**, *578*, 124080. [CrossRef]
18. Dong, Y.; Yuan, H.; Ge, D.; Zhu, N. A Novel Conditioning Approach for Amelioration of Sludge Dewaterability Using Activated Carbon Strengthening Electrochemical Oxidation and Realized Mechanism. *Water Res.* **2022**, *220*, 118704. [CrossRef]
19. Hu, J.; Zhao, L.; Luo, J.; Gong, H.; Zhu, N. A Sustainable Reuse Strategy of Converting Waste Activated Sludge into Biochar for Contaminants Removal from Water: Modifications, Applications and Perspectives. *J. Hazard. Mater.* **2022**, *438*, 129437. [CrossRef] [PubMed]
20. Sun, S.; Liu, H.; Zhang, J.; Wang, W.; Pang, X.; Zhu, X.-G.; Wang, Y.; Wan, S. Application of a Novel Coagulant in Reservoir Water Treatment in Qingdao. *Desalination Water Treat.* **2023**, *284*, 49–60. [CrossRef]
21. Wang, Z.; Hu, L.; Zhao, M.; Dai, L.; Hrynsphan, D.; Savitskaya, T.; Chen, J. Bamboo Charcoal Fused with Polyurethane Foam for Efficiently Removing Organic Solvents from Wastewater: Experimental and Simulation. *Biochar* **2022**, *4*, 28. [CrossRef]
22. Thabede, P.M.; Shooto, N.D.; Xaba, T.; Naidoo, E.B. Magnetite Functionalized Nigella Sativa Seeds for the Uptake of Chromium(VI) and Lead(II) Ions from Synthetic Wastewater. *Adsorpt. Sci. Technol.* **2021**, *2021*, 6655227. [CrossRef]
23. Eze, S.I.; Abugu, H.O.; Odewole, O.A.; Ukwueze, N.N.; Alum, L.O. Thermal and Chemical Pretreatment of Terminalia Mantaly Seed Husk Biosorbent to Enhance the Adsorption Capacity for Pb^{2+}. *Sci. Afr.* **2022**, *15*, e01123. [CrossRef]
24. Castro, D.J.; Rosas-Laverde, N.M.; Aldás, M.B.; Almeida-Naranjo, C.E.; Pruna, A. Chemical Modification of Agro-Industrial Waste-Based Bioadsorbents for Enhanced Removal of Zn(II) Ions from Aqueous Solutions. *Materials* **2021**, *14*, 2134. [CrossRef]
25. Shah, G.M.; Imran, M.; Aiman, U.; Iqbal, M.; Akram, M.; Javeed, H.M.R.; Waqar, A.; Rabbani, F. Efficient Sequestration of Lead from Aqueous Systems by Peanut Shells and Compost: Evidence from Fixed Bed Column and Batch Scale Studies. *PeerJ Phys. Chem.* **2022**, *4*, 21. [CrossRef]
26. Azam, M.; Wabaidur, S.M.; Khan, M.R.; Al-Resayes, S.I.; Islam, M.S. Heavy Metal Ions Removal from Aqueous Solutions by Treated Ajwa Date Pits: Kinetic, Isotherm, and Thermodynamic Approach. *Polymers* **2022**, *14*, 914. [CrossRef] [PubMed]
27. Mariana, M.; Mulana, F.; Juniar, L.; Fathira, D.; Safitri, R.; Muchtar, S.; Bilad, M.R.; Shariff, A.H.M.; Huda, N. Development of Biosorbent Derived from the Endocarp Waste of Gayo Coffee for Lead Removal in Liquid Wastewater—Effects of Chemical Activators. *Sustainability* **2021**, *13*, 3050. [CrossRef]
28. Batool, F.; Akbar, J.; Iqbal, S.; Noreen, S.; Bukhari, S.N.A. Study of Isothermal, Kinetic, and Thermodynamic Parameters for Adsorption of Cadmium: An Overview of Linear and Nonlinear Approach and Error Analysis. *Bioinorg. Chem. Appl.* **2018**, *2018*, 3463724. [CrossRef]
29. Rahman, A.; Yoshida, K.; Islam, M.M.; Kobayashi, G. Investigation of Efficient Adsorption of Toxic Heavy Metals (Chromium, Lead, Cadmium) from Aquatic Environment Using Orange Peel Cellulose as Adsorbent. *Sustainability* **2023**, *15*, 4470. [CrossRef]
30. Suhaimi, N.; Kooh, M.R.R.; Lim, C.M.; Chao, C.-T.C.; Chau, Y.-F.C.; Mahadi, A.H.; Chiang, H.-P.; Hassan, N.H.H.; Thotagamuge, R. The Use of Gigantochloa Bamboo-Derived Biochar for the Removal of Methylene Blue from Aqueous Solution. *Adsorpt. Sci. Technol.* **2022**, *2022*, 8245797. [CrossRef]
31. Kooh, M.R.R.; Dahri, M.K.; Lim, L.B.L. Removal of Methyl Violet 2B Dye from Aqueous Solution Using Nepenthes Rafflesiana Pitcher and Leaves. *Appl. Water Sci.* **2017**, *7*, 3859–3868. [CrossRef]
32. Rahman, A.; Haque, M.A.; Ghosh, S.; Shinu, P.; Attimarad, M.; Kobayashi, G. Modified Shrimp-Based Chitosan as an Emerging Adsorbent Removing Heavy Metals (Chromium, Nickel, Arsenic, and Cobalt) from Polluted Water. *Sustainability* **2023**, *15*, 2431. [CrossRef]
33. Akpomie, K.G.; Conradie, J. Advances in Application of Cotton-Based Adsorbents for Heavy Metals Trapping, Surface Modifications and Future Perspectives. *Ecotoxicol. Environ. Saf.* **2020**, *201*, 110825. [CrossRef] [PubMed]
34. Güzel, F.; Sayğılı, H.; Sayğılı, G.A.; Koyuncu, F.; Yılmaz, C. Optimal Oxidation with Nitric Acid of Biochar Derived from Pyrolysis of Weeds and Its Application in Removal of Hazardous Dye Methylene Blue from Aqueous Solution. *J. Clean. Prod.* **2017**, *144*, 260–265. [CrossRef]
35. Wei, S.; Chen, T.; Hou, H.; Xu, Y. Recent Advances in Electrochemical Sterilization. *J. Electroanal. Chem.* **2023**, *937*, 117419. [CrossRef]
36. Yang, H.; Li, F.; Hu, N.; Fu, S.-Y. Frictional Characteristics of Graphene Oxide-Modified Continuous Glass Fiber Reinforced Epoxy Composite. *Compos. Sci. Technol.* **2022**, *223*, 109446. [CrossRef]
37. Chen, D.; Wang, Q.; Li, Y.; Li, Y.; Zhou, H.; Yue, F. A General Linear Free Energy Relationship for Predicting Partition Coefficients of Neutral Organic Compounds. *Chemosphere* **2020**, *247*, 125869. [CrossRef]
38. Sikam, K.G.; Dzouemo, L.C.; Happi, G.M.; Wansi, J.D. Recent advances on pharmacology and chemistry of *Pycnanthus angolensis* Over the last decade (2012–2021). *Nat. Resour. Hum. Health* **2022**, *2*, 322–326. [CrossRef] [PubMed]
39. Simic, A.; Kroepfl, D.; Simic, N.; Ogunwande, I.A. *Pycnanthus angolensis* (Welw) Excell: Volatile Oil Constituents and Antimicrobial Activity. *Nat. Prod. Commun.* **2006**, *1*, 651–654. [CrossRef]
40. Bello, O.A.; Akinyele, A.O. Qualitative morphology of *Pycnanthus angolensis* (Welw.) fruits and seeds. *Afr. J. Agric. Technol. Environ.* **2018**, *7*, 90–98.
41. Oladimeji, O.; Ahmadu, A.A. Antioxidant activity of compounds isolated from *Pycnanthus angolensis* (Welw.) Warb and *Byrophyllum pinnatum* (Lam.) Oken. *Eur. Chem. Bull.* **2019**, *8*, 96–100. [CrossRef]

42. Gustafson, K.; Wu, Q.; Asante-Dartey, J.; Simon, J.E. Pycnanthus angolensis: Bioactive Compounds and Medicinal Applications. In *African Natural Plant Products Volume II: Discoveries and Challenges in Chemistry, Health, and Nutrition*; ACS Symposium Series; American Chemical Society: Washington, DC, USA, 2013; pp. 63–78. [CrossRef]
43. Guo, B.; Wang, Y.; Yu, F.; Liang, C.; Li, T.; Yao, X.; Hu, F. The Effects of Environmental Tax Reform on Urban Air Pollution: A Quasi-Natural Experiment Based on the Environmental Protection Tax Law. *Front. Public Health* **2022**, *10*, 967524. [CrossRef] [PubMed]
44. Song, Z.; Han, D.; Yang, M.; Huang, J.; Shao, X.; Li, H. Formic Acid Formation via Direct Hydration Reaction (CO + $H_2O \rightarrow$ HCOOH) on Magnesia-Silver Composite. *Appl. Surf. Sci.* **2023**, *607*, 155067. [CrossRef]
45. Zhang, G.; Zhao, Z.; Yin, X.; Zhu, Y. Impacts of Biochars on Bacterial Community Shifts and Biodegradation of Antibiotics in an Agricultural Soil during Short-Term Incubation. *Sci. Total Environ.* **2021**, *771*, 144751. [CrossRef]
46. Imran, M.; Khan, Z.U.H.; Iqbal, M.; Iqbal, J.; Shah, N.S.; Munawar, S.; Ali, S.; Murtaza, B.; Naeem, M.A.; Rizwan, M. Effect of Biochar Modified with Magnetite Nanoparticles and HNO_3 for Efficient Removal of Cr(VI) from Contaminated Water: A Batch and Column Scale Study. *Environ. Pollut.* **2020**, *261*, 114231. [CrossRef]
47. Diraki, A.; Mackey, H.R.; McKay, G.; Abdala, A. Removal of Oil from Oil–Water Emulsions Using Thermally Reduced Graphene and Graphene Nanoplatelets. *Chem. Eng. Res. Des.* **2018**, *137*, 47–59. [CrossRef]
48. Tariq, M.; Nadeem, M.; Iqbal, M.; Imran, M.; Siddique, M.H.; Iqbal, Z.; Amjad, M.; Rizwan, M.; Ali, S. Effective Sequestration of Cr (VI) from Wastewater Using Nanocomposite of ZnO with Cotton Stalks Biochar: Modeling, Kinetics, and Reusability. *Environ. Sci. Pollut. Res.* **2020**, *27*, 33821–33834. [CrossRef]
49. Waqar, R.; Kaleem, M.; Iqbal, J.; Minhas, L.A.; Haris, M.S.; Chalgham, W.; Ahmad, A.; Mumtaz, A.S. Kinetic and Equilibrium Studies on the Adsorption of Lead and Cadmium from Aqueous Solution Using *Scenedesmus* sp. *Sustainability* **2023**, *15*, 6024. [CrossRef]
50. Dada, A.O.; Olalekan, A.P.; Olatunya, A.M.; Dada, O.J.I.J.C. Langmuir, Freundlich, Temkin and Dubinin-Radushkevich Isotherms Studies of Equilibrium Sorption of Zn^{2+} unto Phosphoric Acid Modified Rice Husk. *IOSR J. Appl. Chem.* **2012**, *3*, 38–45. [CrossRef]
51. Shahbeig, H.; Bagheri, N.; Ghorbanian, S.A.; Hallajisani, A.; Pourkarimi, S. A new adsorption isotherm model of aqueous solutions on granular activated carbon. *World J. Model. Simul.* **2013**, *9*, 243–254.
52. Theivarasu, C.; Mylsamy, S. Removal of Malachite Green from Aqueous Solution by Activated Carbon Developed from Cocoa (*Theobroma Cacao*) Shell—A Kinetic and Equilibrium Studies. *J. Chem.* **2011**, *8*, S363–S371. [CrossRef]
53. Israel, U.; Eduok, U. Biosorption of zinc from aqueous solution using coconut (*Cocos nucifera* L) coir dust. *Arch. Appl. Sci. Res.* **2012**, *4*, 809–819.
54. Amin, M.; Alazba, A.A.; Shafiq, M. Adsorptive Removal of Reactive Black 5 from Wastewater Using Bentonite Clay: Isotherms, Kinetics and Thermodynamics. *Sustainability* **2015**, *7*, 15302–15318. [CrossRef]
55. Akpomie, K.G.; Conradie, J. Ultrasonic Aided Sorption of Oil from Oil-in-Water Emulsion onto Oleophilic Natural Organic-Silver Nanocomposite. *Chem. Eng. Res. Des.* **2021**, *165*, 12–24. [CrossRef]
56. Ezekoye, O.M.; Akpomie, K.G.; Eze, S.I.; Chukwujindu, C.N.; Ani, J.U.; Ujam, O.T. Biosorptive Interaction of Alkaline Modified *Dialium Guineense* Seed Powders with Ciprofloxacin in Contaminated Solution: Central Composite, Kinetics, Isotherm, Thermodynamics, and Desorption. *Int. J. Phytoremediat.* **2020**, *22*, 1028–1037. [CrossRef]
57. Ayawei, N.; Ebelegi, A.N.; Wankasi, D. Modelling and Interpretation of Adsorption Isotherms. *J. Chem.* **2017**, *2017*, 3039817. [CrossRef]
58. Eze, S.I.; Abugu, H.O.; Ekowo, L.C. Thermal and Chemical Pretreatment of Cassia Sieberiana Seed as Biosorbent for Pb^{2+} Removal from Aqueous Solution. *Desalination Water Treat.* **2021**, *226*, 223–241. [CrossRef]
59. Beksissa, R.; Tekola, B.; Ayala, T.; Dame, B. Investigation of the Adsorption Performance of Acid Treated Lignite Coal for Cr (VI) Removal from Aqueous Solution. *Environ. Chall.* **2021**, *4*, 100091. [CrossRef]
60. Tan, C.-Y.; Gan, L.; Lu, X.; Chen, Z. Biosorption of Basic Orange Using Dried A. Filiculoides. *Ecol. Eng.* **2010**, *36*, 1333–1340. [CrossRef]
61. Fonseca, J.G.; Albis, A.; Montenegro, A.R. Evaluation of Zinc Adsorption Using Cassava Peels (Manihot Esculenta) Modified with Citric Acid. *Contemp. Eng. Sci.* **2018**, *11*, 3575–3585. [CrossRef]
62. Khan, M.A.; Otero, M.; Kazi, M.; Alqadami, A.A.; Wabaidur, S.M.; Siddiqui, M.R.; Alothman, Z.A.; Sumbul, S. Unary and Binary Adsorption Studies of Lead and Malachite Green onto a Nanomagnetic Copper Ferrite/Drumstick Pod Biomass Composite. *J. Hazard. Mater.* **2019**, *365*, 759–770. [CrossRef]
63. Li, X.; Tang, Y.; Cao, X.; Lu, D.; Luo, F.; Shao, W. Preparation and Evaluation of Orange Peel Cellulose Adsorbents for Effective Removal of Cadmium, Zinc, Cobalt and Nickel. *Colloids Surf. A Physicochem. Eng. Asp.* **2008**, *317*, 512–521. [CrossRef]
64. Ahmad, M.; Ahmad, M.; Usman, A.R.A.; Al-Faraj, A.S.; Abduljabbar, A.S.; Al-Wabel, M.I. Biochar Composites with Nano Zerovalent Iron and Eggshell Powder for Nitrate Removal from Aqueous Solution with Coexisting Chloride Ions. *Environ. Sci. Pollut. Res.* **2017**, *25*, 25757–25771. [CrossRef]
65. Shafiq, M.; Alazba, A.A.; Amin, M. Kinetic and Isotherm Studies of Ni^{2+} and Pb^{2+} Adsorption from Synthetic Wastewater Using Eucalyptus Camdulensis—Derived Biochar. *Sustainability* **2021**, *13*, 3785. [CrossRef]
66. Das, D.; Samal, D.P.; Bc, M. Preparation of Activated Carbon from Green Coconut Shell and Its Characterization. *J. Chem. Eng. Process Technol.* **2015**, *6*, 248. [CrossRef]

67. Agarry, S.E.; Ogunleye, O.O.; Ajani, O.A. Biosorptive Removal of Cadmium (II) Ions from Aqueous Solution by Chemically Modified Onion Skin: Batch Equilibrium, Kinetic and Thermodynamic Studies. *Chem. Eng. Commun.* **2015**, *202*, 655–673. [CrossRef]
68. Adetoye, M.D.; Adeojo, S.O.; Ajiboshin, B.F. Photocatalyst utilization of garlic waste as adsorbentfor heavy metal removal from aqueous solution. *J. Pure Appl. Sci.* **2018**, *6*, 6–13.
69. Zhou, P.; Regenstein, J.M. Effects of Alkaline and Acid Pretreatments on Alaska Pollock Skin Gelatin Extraction. *J. Food Sci.* **2006**, *70*, c392–c396. [CrossRef]
70. Yusuff, A.S. Adsorptive Removal of Lead and Cadmium Ions from Aqueous Solutions by Aluminium Oxide Modified Onion Skin Wastes: Adsorbent Characterization, Equilibrium Modelling and Kinetic Studies. *Energy Environ.* **2021**, *33*, 152–169. [CrossRef]
71. Huang, J.; Fang, Y.; Zeng, G.; Xue, L.; Gu, Y.; Shi, L.; Liu, W.; Shi, Y. Influence of PH on Heavy Metal Speciation and Removal from Wastewater Using Micellar-Enhanced Ultrafiltration. *Chemosphere* **2017**, *173*, 199–206. [CrossRef]
72. Tang, S.; Lin, L.-C.; Wang, X.; Yu, A.; Sun, X. Interfacial Interactions between Collected Nylon Microplastics and Three Divalent Metal Ions (Cu(II), Ni(II), Zn(II)) in Aqueous Solutions. *J. Hazard. Mater.* **2021**, *403*, 123548. [CrossRef] [PubMed]
73. Awual, M.R.; Hasan, M.M.; Eldesoky, G.E.; Khaleque, M.A.; Rahman, M.M.; Naushad, M. Facile Mercury Detection and Removal from Aqueous Media Involving Ligand Impregnated Conjugate Nanomaterials. *Chem. Eng. J.* **2016**, *290*, 243–251. [CrossRef]
74. Wang, R.-S.; Li, Y.; Shuai, X.; Liang, R.; Chen, J.; Liu, C. PEctin/Activated Carbon-Based Porous Microsphere for PB^{2+} Adsorption: Characterization and Adsorption Behaviour. *Polymers* **2021**, *13*, 2453. [CrossRef] [PubMed]
75. Radha, E.; Gomathi, T.; Sudha, P.N.; Latha, S.; Ghfar, A.A.; Hossain, N. Adsorption Studies on Removal of Pb(II) and Cd(II) Ions Using Chitosan Derived Copoymeric Blend. *Biomass Convers. Biorefin.* **2021**. [CrossRef]
76. Taşar, Ş.; Kaya, F.; Özer, A. Biosorption of Lead(II) Ions from Aqueous Solution by Peanut Shells: Equilibrium, Thermodynamic and Kinetic Studies. *J. Environ. Chem. Eng.* **2014**, *2*, 1018–1026. [CrossRef]
77. Thi, T.T.L.; Van, K. Adsorption behavior of Pb (II) in aqueous solution using coffee husk-based activated carbon modified by nitric acid. *Am. J. Eng. Res.* **2016**, *5*, 120–129.
78. Tangtubtim, S.; Saikrasun, S. Adsorption Behavior of Polyethyleneimine-Carbamate Linked Pineapple Leaf Fiber for Cr(VI) Removal. *Appl. Surf. Sci.* **2019**, *467–468*, 596–607. [CrossRef]
79. Ghanim, B.; Leahy, J.J.; O'Dwyer, T.F.; Pembroke, J.T.; Murnane, J.G. Removal of Hexavalent Chromium (Cr(VI)) from Aqueous Solution Using Acid-modified Poultry Litter derived Hydrochar: Adsorption, Regeneration and Reuse. *J. Chem. Technol. Biotechnol.* **2021**, *97*, 55–66. [CrossRef]
80. Chukwuemeka-Okorie, H.O.; Ekuma, F.K.; Akpomie, K.G.; Nnaji, J.C.; Okereafor, A.G. Adsorption of Tartrazine and Sunset Yellow Anionic Dyes onto Activated Carbon Derived from Cassava Sievate Biomass. *Appl. Water Sci.* **2021**, *11*, 27. [CrossRef]
81. Wei, W.; Li, A.; Ma, F.; Pi, S.; Yang, J.; Wang, Q.; Ni, B.-J. Simultaneous Sorption and Reduction of Cr(VI) in Aquatic System by Microbial Extracellular Polymeric Substances from Klebsiella Sp. J1. *J. Chem. Technol. Biotechnol.* **2018**, *93*, 3152–3159. [CrossRef]
82. Cui, D.; Tan, C.; Deng, H.; Gu, X.; Pi, S.; Chen, T.; Zhou, L.; Li, A. Biosorption Mechanism of Aqueous Pb^{2+}, Cd^{2+}, and Ni^{2+} Ions on Extracellular Polymeric Substances (EPS). *Archaea* **2020**, *2020*, 8891543. [CrossRef]
83. Hu, L.; Guang, C.; Liu, Y.; Su, Z.; Gong, S.; Yao, Y.; Wang, Y. Adsorption Behavior of Dyes from an Aqueous Solution onto Composite Magnetic Lignin Adsorbent. *Chemosphere* **2020**, *246*, 125757. [CrossRef]
84. Liu, X.; Xu, X.; Dong, X.; Park, J. Competitive Adsorption of Heavy Metal Ions from Aqueous Solutions onto Activated Carbon and Agricultural Waste Materials. *Pol. J. Environ. Stud.* **2019**, *29*, 749–761. [CrossRef]
85. Ghanim, B.; Murnane, J.G.; O'Donoghue, L.M.T.; Courtney, R.; Pembroke, J.T.; O'Dwyer, T.F. Removal of Vanadium from Aqueous Solution Using a Red Mud Modified Saw Dust Biochar. *J. Water Process Eng.* **2020**, *33*, 101076. [CrossRef]
86. Shi, Y.; Zhang, T.; Ren, H.; Kruse, A.; Cui, R. Polyethylene Imine Modified Hydrochar Adsorption for Chromium (VI) and Nickel (II) Removal from Aqueous Solution. *Bioresour. Technol.* **2018**, *247*, 370–379. [CrossRef] [PubMed]
87. Dehmani, Y.; Sellaoui, L.; Al-Ghamdi, Y.O.; Lainé, J.; Badawi, M.; Amhoud, A.; Bonilla-Petriciolet, A.; Lamhasni, T.; Abouarnadasse, S. Kinetic, Thermodynamic and Mechanism Study of the Adsorption of Phenol on Moroccan Clay. *J. Mol. Liq.* **2020**, *312*, 113383. [CrossRef]
88. Barros, L.; Carvalho, A.M.; Ferreira, I.C.F.R. The Nutritional Composition of Fennel (Foeniculum Vulgare): Shoots, Leaves, Stems and Inflorescences. *Lebensm.-Wiss. Technol.* **2010**, *43*, 814–818. [CrossRef]
89. Anwar, J.; Shafique, U.; Waheed-Uz-Zaman; Salman, M.; Dar, A.; Anwar, S. Removal of Pb(II) and Cd(II) from Water by Adsorption on Peels of Banana. *Bioresour. Technol.* **2010**, *101*, 1752–1755. [CrossRef]
90. Gupta, V.K.; Ali, I. Removal of Lead and Chromium from Wastewater Using Bagasse Fly Ash—A Sugar Industry Waste. *J. Colloid Interface Sci.* **2004**, *271*, 321–328. [CrossRef]
91. Peláez-Cid, A.-A.; Romero-Hernández, V.; Herrera-González, A.M.; Bautista-Hernández, A.; Coreño-Alonso, O. Synthesis of Activated Carbons from Black Sapote Seeds, Characterization and Application in the Elimination of Heavy Metals and Textile Dyes. *Chin. J. Chem. Eng.* **2020**, *28*, 613–623. [CrossRef]
92. Lalhruaitluanga, H.; Jayaram, K.M.; Prasad, M.N.V.; Kumar, K.K. Lead(II) Adsorption from Aqueous Solutions by Raw and Activated Charcoals of *Melocanna baccifera* Roxburgh (Bamboo)—A Comparative Study. *J. Hazard. Mater.* **2010**, *175*, 311–318. [CrossRef] [PubMed]
93. Shukla, S.R.; Pai, R.S. Removal of Pb(II) from Solution Using Cellulose-Containing Materials. *J. Chem. Technol. Biotechnol.* **2005**, *80*, 176–183. [CrossRef]

94. Gaur, N.; Kukreja, A.; Yadav, M.; Tiwari, A. Adsorptive Removal of Lead and Arsenic from Aqueous Solution Using Soya Bean as a Novel Biosorbent: Equilibrium Isotherm and Thermal Stability Studies. *Appl. Water Sci.* **2018**, *8*, 98. [CrossRef]
95. Abugu, H.O.; Okoye, P.A.C.; Ajiwe, V.I.E.; Omuku, P.E.; Umeobika, U.C. Preparation and Characterization of Activated Carbon Produced from Oil Bean (Ugba or Ukpaka) and Snail Shell. *J. Environ. Anal. Chem.* **2015**, *2*, 165. [CrossRef]
96. Chijioke, U.; Benjamin, D.; Anayochukwu, E.; Onyeka, A.; Ogechi, A.; Ifeanyi, S.; Abiola, O. Chromium Adsorption Using Modified Locust Bean and Maize Husk. *Pharma Chem.* **2020**, *12*, 7–14.
97. Abugu, H.O.; Okoye, P.A.C.; Ajiwe, V.I.E.; Ofordile, P.C. Preparation and Characterisation of Activated Carbon from Agrowastes Peanut Seed (African Canarium) and Palm Kernel Shell. *Int. J. Innov. Res. Dev.* **2014**, *3*, 418–441.